

Collider Signatures for Heavy Lepton Triplet in Type I+III Seesaw

Abdesslam Arhrib,¹ Borut Bajc,² Dilip Kumar Ghosh,³

Tao Han,⁴ Gui-Yu Huang,⁵ Ivica Puljak,⁶ and Goran Senjanović⁷

¹*Département de Mathématiques, Faculté des Sciences et Techniques*

B.P 416 Tanger, Morocco

²*J. Stefan Institute, 1000 Ljubljana, Slovenia*

³*Department of Theoretical Physics and Centre for Theoretical Sciences*

Indian Association for the Cultivation of Science

2A & 2B Raja S.C. Mullick Road, Kolkata 700 032, India

⁴*Department of Physics, University of Wisconsin, Madison, WI 53706, USA*

⁵*Department of Physics, University of California, Davis, CA 95616, USA*

⁶*FESB, University of Split, Split, Croatia*

⁷*International Centre for Theoretical Physics, Trieste, Italy*

Abstract

The minimal SU(5) theory augmented by the fermionic adjoint representation restores the coupling constant unification and gives realistic neutrino masses and mixing through the hybrid Type I and Type III seesaw. The crucial prediction of the theory is an SU(2) lepton triplet with the mass below TeV. We study the signature of these heavy leptons and propose the strategy to test this mechanism at the hadron and lepton colliders. The smoking gun evidence of the theory is $\Delta L = 2$ lepton number violation through events of a pair of like-sign leptons plus four jets without significant missing energy at hadron colliders. We find that via this unique channel, the heavy lepton can be searched for up to a mass of 200 GeV at the Tevatron with 8 fb^{-1} , and up to 450 (700) GeV at the LHC of 14 TeV C.M. energy with 10 (100) fb^{-1} . The signal rate at the 10 TeV LHC is reduced to 60% – 35% for a mass of 200–700 GeV. We also comment on how to distinguish this theory from other models with similar heavy leptons. Finally, we compare the production rates and angular distributions of heavy leptons in e^+e^- collisions for various models.

I. INTRODUCTION

Within the context of the Standard Model (SM), neutrino masses require the presence of the higher dimensional operator, symbolically written as [1]

$$\mathcal{L}_{eff} = y_{eff} \frac{LLHH}{M}, \quad (1)$$

where L is the usual leptonic doublet $L = (\nu, e)_L$, H is the standard model Higgs doublet $H = (h^+, h^0)$, and y_{eff} is an effective Yukawa coupling. This operator breaks the lepton number by two units ($\Delta L = 2$). Once the electroweak symmetry is spontaneously broken by the Higgs vacuum expectation value (v), neutrinos get Majorana masses

$$m_\nu = y_{eff} \frac{v^2}{M}. \quad (2)$$

The smallness of neutrino masses from the observation tells us that either M is very large $M \gg v$, or y_{eff} must be small, both cases equally natural from the technical point of view.

Observation of the lepton number violation would be the definitive test for the generation of neutrino Majorana masses as in Eq. (1). However, if we wish to understand the operator to a better level or to derive m_ν , we need a completion of the SM which leads to Eq. (1). There are three possible extensions [2] to the SM which, after integrating out the new heavy states, will lead to Eq. (1):

1. fermionic singlets, called right-handed neutrinos; this is called Type I seesaw [3];
2. a scalar $SU(2)_L$ triplet ($Y = 2$); this is called Type II seesaw [4, 5, 6];
3. a fermionic $SU(2)_L$ triplet ($Y = 0$) called Type III seesaw [7].

The Type I and Type II seesaw scenarios have been studied in depth in the literature, while the Type III exploration is somewhat limited. This is quite natural since Types I and II are predicted in left-right symmetric theories, and thus can be incorporated in a predictive grand unified theory based on $SO(10)$. The inclusion of right-handed neutrinos offers the simplest possibility of gauging the anomaly free $B - L$ accidental symmetry of the SM, and the Higgs triplet provides the simplest way of generating their masses [6] in L-R symmetric theories [8, 9, 10, 11].

It is tempting to address the issue of M in the context of the minimal $SU(5)$, which is known to have failed for two profound reasons: the gauge couplings do not unify and

neutrinos are massless. A simple way of curing both is to add an adjoint 24_F fermionic representation [12]. Neutrino masses result from the mixture of Type I and Type III seesaw since 24_F contains both the singlet S and the triplet T , with an interesting prediction of one massless neutrino. Even more interestingly, the unification constraints force the triplet to be light: $M_T \lesssim 1$ TeV. In short, we have a predictive grand unified theory that can be tested in future experiments. This motivates us to study the observability of the fermionic triplet with the predicted characteristics in the collider experiments.

We should stress that minimality plays a crucial role in the physics of the triplet. If, and only if minimality is assumed, the triplet is predicted to be light and to be a source of neutrino mass. For example, we are not allowed to add right-handed neutrinos as $SU(5)$ singlets and any higher dimensional operator should be suppressed by a cutoff above M_{GUT} . As a consequence the theory does not allow for more generations, for otherwise the fourth generation neutral lepton is forced to be another light neutrino. The higher dimensional operator would give an infinitesimal mass, and since there is no room for seesaw, this particle would be effectively massless.

We calculate the production rate and subsequent decays of the triplet fermion responsible for Type III seesaw at hadron colliders. We focus on the gold-plated events: the $\Delta L = 2$ channels, of same-sign dileptons accompanied by multiple jets without significant missing transverse energy. These events as originally discussed a long time ago [13] offer a possibility of directly observing the Majorana nature of the neutral triplet lepton and are characteristic of the seesaw mechanism that leads to Majorana light neutrinos.

This was already studied for the LHC [14, 15, 16, 17] for the seesaw with three triplets. In our case we are dealing with a well defined theory with further constraints: a single triplet in the TeV region and one massless neutrino. In particular, we establish the correlations between the lepton flavors in the LHC signal and the neutrino mass patterns. The decays of the triplet are characterized by the same Yukawa couplings that enter into the neutrino mass matrix and so the collider signatures can be of great help in determining the rest of the neutrino mixings and phases.

It is worth emphasizing that the textbook example of $\Delta L = 2$ violation, the neutrinoless double beta decay, depends on the nature of the seesaw completion of the standard model and thus by itself cannot point to the origin of the Majorana neutrino mass.

The rest of this paper is organized as follows. In section II we describe the salient features

of the SU(5) theory with an adjoint fermion. We briefly review the unification analysis which forces the triplet to be light, below TeV. In Sec. III, we then explore the constraints on the model parameters based on the neutrino oscillation experiments. We find interesting correlations between the couplings and the neutrino mass patterns. In Sec. IV, we study the decays of the fermionic triplet. We once again present the correlations between the decay branching fractions and the neutrino mass and the possible Majorana phases. Section V is the core of our paper. Here we carefully discuss the smoking gun predictions of the theory: same-sign dilepton plus four jets without significant missing energy. We estimate the SM backgrounds and develop the strategies to separate the signal from backgrounds. We discuss the discovery potential of both the Tevatron and LHC and demonstrate that the Tevatron could probe the lepton triplet up to a mass 200 GeV with a 8 fb^{-1} integrated luminosity, while the LHC could probe the triplets up to a mass 450 (700) GeV with a luminosity of 10 (100) fb^{-1} . We also calculate the signal rate at the 10 TeV LHC. In particular, we provide some general remarks on how to distinguish the lepton triplet from other heavy leptonic states. As a complementary study in this regard, we present in Sec. VI the results for cross sections and distributions at an e^+e^- Linear collider for a few representative models. Finally, in Sec. VII, we conclude with a critical discussion and outlook.

II. SU(5) WITH AN ADJOINT FERMION

A practitioner of grand unification is faced with an embarrassing problem: after more than three decades we still do not have a prototype, minimal working model that is phenomenologically acceptable at low energies. We actually had one for a while: the original theory of Georgi and Glashow [18], the so called minimal SU(5). It worked great when neutrinos could have been massless and when the wrong measurement of $\sin^2 \theta_W$ indicated the unification of gauge couplings of the SM. Today we know that the theory must be changed and if you are willing to make a brave assumption of super split supersymmetry [19], a particularly elegant and simple modification is to add an adjoint fermionic 24_F .¹ The resulting predictions are remarkable [12, 22]:

1. The triplet mass must be small: $M_T \lesssim 1 \text{ TeV}$, in order to keep the proton stable

¹ Another possibility would be to add a scalar 15-dimensional representation [20, 21].

enough;

2. For a very light triplet, close to its lower limit of about 100 GeV, the GUT scale reaches its maximum of 10^{16} GeV, and falls off with increasing M_T . A non observation of the triplet would guarantee seeing the proton decay in the next generation of experiments;
3. The triplet decays through the same lepton number violating Yukawa couplings that enters the seesaw formula;
4. The theory is consistent if and only if there are three generations. As already discussed in the introduction, minimality arguments prevents the hypothetical fourth generation neutrino to get a mass bigger than $M_Z/2$;
5. One light neutrino remains massless;
6. The scalar triplet is also possibly light.

This is an example of a predictive grand unified theory that offers a possibility of observing the seesaw mechanism at colliders. The seesaw, in this case of both Type I and III, results from the Yukawa couplings of the singlet S and triplet T fermions from the adjoint 24_F

$$\mathcal{L}_Y(\nu) = y_S^i L_i H S + y_T^i L_i H T - \frac{M_S}{2} S S - \frac{M_T}{2} T T + h.c. \quad (3)$$

where the index i refers to the flavors defined with respect to the charged leptons.

After the $SU(2)_L \times U(1)$ symmetry breaking $\langle H \rangle = v \approx 174$ GeV, one obtains in the usual manner the light neutrino mass matrix upon integrating out S and T

$$m_\nu^{ij} = -v^2 \left(\frac{y_T^i y_T^j}{M_T} + \frac{y_S^i y_S^j}{M_S} \right) \quad (4)$$

with $M_T \lesssim 1$ TeV and M_S undetermined. For an alternative version of the electroweak seesaw see for example [23] with light doublets instead of a triplet.²

The neutrino mass matrix in Eq. (4) is clearly rank 2, thus one massless neutrino. This is simply a reflection of the fact that there are only two heavy neutral leptons, T^0 and S . Of course, there may be a higher dimensional operator as in Eq. (1) which will lift the zero

² Light doublets are predicted with unification arguments also in minimal walking technicolor [24], while a light triplet in [25].

mass eigenvalue, but for $M > M_{GUT}$ it is less than 10^{-4} eV, thus completely negligible. For simplicity we will keep referring to the lightest neutrino as being massless. The main point is that we have a hierarchical spectrum of neutrinos, and neutrino masses are known up to the normal (NH) versus inverted (IH) hierarchy ambiguity.

In short, the SU(5) theory augmented with an adjoint fermion can be said to keep the ugliness of the minimal theory: asymmetric fermionic representations and the fine-tuning, but also its remarkable predictiveness. It offers serious hope for the observation of the proton decay in the next generation of experiments, but in contrast with the minimal theory it predicts a few oasis in the desert, the first one in the form of the fermion SU(2) triplet, at the energies accessible by the current and next generation high-energy colliders. We now turn to its implications for neutrino physics.

III. NEUTRINO PARAMETER CONSTRAINTS

To make a direct contact with observables, it is necessary to connect the model parameters with the neutrino masses and the mixing angles. We first note the relations for the neutrino mass parameters with the normal hierarchy (NH: $m_3^\nu > m_1^\nu = 0$)

$$m_1^\nu = 0, \quad m_2^\nu = \sqrt{\Delta m_S^2}, \quad m_3^\nu = \sqrt{\Delta m_A^2 + \Delta m_S^2}, \quad (5)$$

and the inverted hierarchy (IH: $0 = m_3^\nu < m_1^\nu$)

$$m_1^\nu = \sqrt{\Delta m_A^2 - \Delta m_S^2}, \quad m_2^\nu = \sqrt{\Delta m_A^2}, \quad m_3^\nu = 0, \quad (6)$$

where we take the neutrino mass parameters [26] as measured in the solar and atmospheric oscillation experiments

$$\Delta m_S^2 \approx 7.7 \times 10^{-5} \text{ eV}^2, \quad \Delta m_A^2 \approx 2.4 \times 10^{-3} \text{ eV}^2. \quad (7)$$

Since one neutrino is massless in our model, the neutrino flavor mixing matrix has only one physical Majorana phase Φ

$$U = \begin{pmatrix} c_{12}c_{13} & s_{12}c_{13} & s_{13}e^{-i\delta} \\ -s_{12}c_{23} - c_{12}s_{23}s_{13}e^{i\delta} & c_{12}c_{23} - s_{12}s_{23}s_{13}e^{i\delta} & s_{23}c_{13} \\ s_{12}s_{23} - c_{12}c_{23}s_{13}e^{i\delta} & -c_{12}s_{23} - s_{12}c_{23}s_{13}e^{i\delta} & c_{23}c_{13} \end{pmatrix} \times \text{diag}(1, e^{i\Phi}, 1). \quad (8)$$

It is useful to invert the seesaw formula (4) following [27, 28] and to parameterize the Yukawa couplings by only one complex parameter.³ We thus have the relations

$$vy_T^{i*} = \begin{cases} i\sqrt{M_T} (U_{i2}\sqrt{m_2^\nu} \cos z + U_{i3}\sqrt{m_3^\nu} \sin z), & \text{NH} \quad (m_1^\nu = 0), \\ i\sqrt{M_T} (U_{i1}\sqrt{m_1^\nu} \cos z + U_{i2}\sqrt{m_2^\nu} \sin z), & \text{IH} \quad (m_3^\nu = 0), \end{cases} \quad (9)$$

and

$$vy_S^{i*} = \begin{cases} -i\sqrt{M_S} (U_{i2}\sqrt{m_2^\nu} \sin z - U_{i3}\sqrt{m_3^\nu} \cos z), & \text{NH} \quad (m_1^\nu = 0), \\ -i\sqrt{M_S} (U_{i1}\sqrt{m_1^\nu} \sin z - U_{i2}\sqrt{m_2^\nu} \cos z), & \text{IH} \quad (m_3^\nu = 0). \end{cases} \quad (10)$$

There is another solution with the opposite sign of the second terms in (9), (10). The major advantage of this parameterization is to allow us to untangle the contributions of y_T and y_S , so that one can separately explore the correlations between these Yukawa couplings and the neutrino oscillation parameters, as we will demonstrate next.

The singlet Yukawa couplings y_S are less useful for our consideration since one does not expect the singlet to be produced at the LHC. The Yukawa couplings $|y_T^i|$ are invariant under the operations

$$y_T^i \rightarrow -y_T^i \quad \text{under} \quad \text{Re}(z) \rightarrow \text{Re}(z) + \pi \quad (11)$$

$$y_T^i \rightarrow -y_T^i \quad \text{under} \quad \Phi \rightarrow \Phi + \pi, \quad z \rightarrow -z \quad (12)$$

$$y_T^i \rightarrow -(y_T^i)^* \quad \text{under} \quad \Phi \rightarrow -\Phi, \quad \delta \rightarrow -\delta, \quad z \rightarrow z^*. \quad (13)$$

It suffices therefore to explore effects of the full range of neutrino parameters by restricting to

$$\text{Im}(z) \geq 0, \quad \Phi \in [-\pi/2, \pi/2], \quad \text{Re}(z) \in [0, \pi]. \quad (14)$$

If we scan over the whole parameter space, this range covers also the other solution to the seesaw equation, Eq. (4), i.e. Eqs. (9) and (10) with the opposite sign of the second term.

It is convenient to introduce a dimensionless parameter a_T , defined as,

$$a_T^i \equiv |y_T^i| \sqrt{\frac{v}{2M_T}}, \quad (15)$$

where $i = 1, 2, 3$ refers to the lepton flavors e, μ, τ . There exist significant constraints on the Yukawa couplings, or on a_T^i , from the low energy data, most notably by various flavor violating processes, such as $\mu \rightarrow 3e$ and lepton universality at the Z -pole [30, 31, 32, 33].

³ For a review on the general rank two neutrino mass, see for example [29].

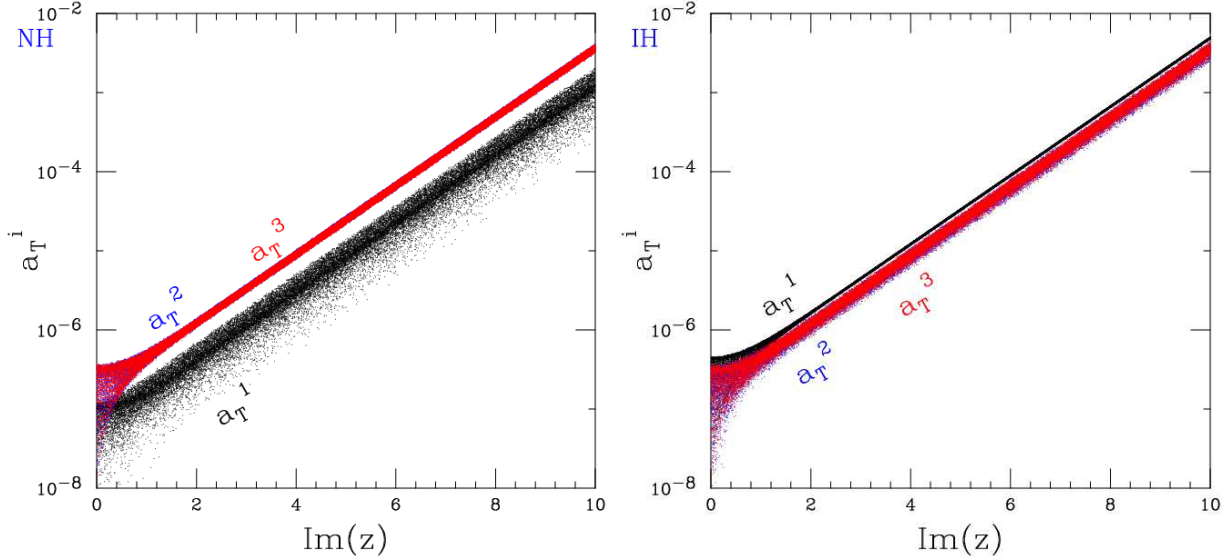


FIG. 1: a_T^i versus $\text{Im}(z)$ for NH (left) and IH (right). $\Phi = 0$.

These limits are intercorrelated and become of order 1% when only one such coupling is nonzero. To be on the safe side hereafter we stick to

$$a_T^i \leq 10^{-2}. \quad (16)$$

We take the experimental lower bound for the triplet mass to be 100 GeV from [34] (although strictly speaking it is found for charged lepton doublets, a similar limit applies for charged triplet). The neutrino mass and mixing constraints are of essential importance in our consideration. We adopt their numerical values from the 2σ fitting in a recent analysis [26].

Based on the relations between our model parameters and the oscillation data, one can predict the size of the couplings in terms of the other parameters. We perform a comprehensive scan over the large parameter space, including both the neutrino oscillation parameters and the theory parameters. The expression of Eq. (9) makes the Yukawa couplings transparent in terms of the complex parameter z . The real part of z leads to a simple oscillatory nature. It is the imaginary part of z that affects the size of the coupling a_T most. This is plotted in Fig. 1 for the NH (left panel) and the IH (right panel), when ignoring the influence of the Majorana phase Φ . Several features are transparent: (a). The Yukawa couplings y_T^i are exponentially enhanced over $\text{Im}(z)$; (b). At large values of $\text{Im}(z)$, the couplings

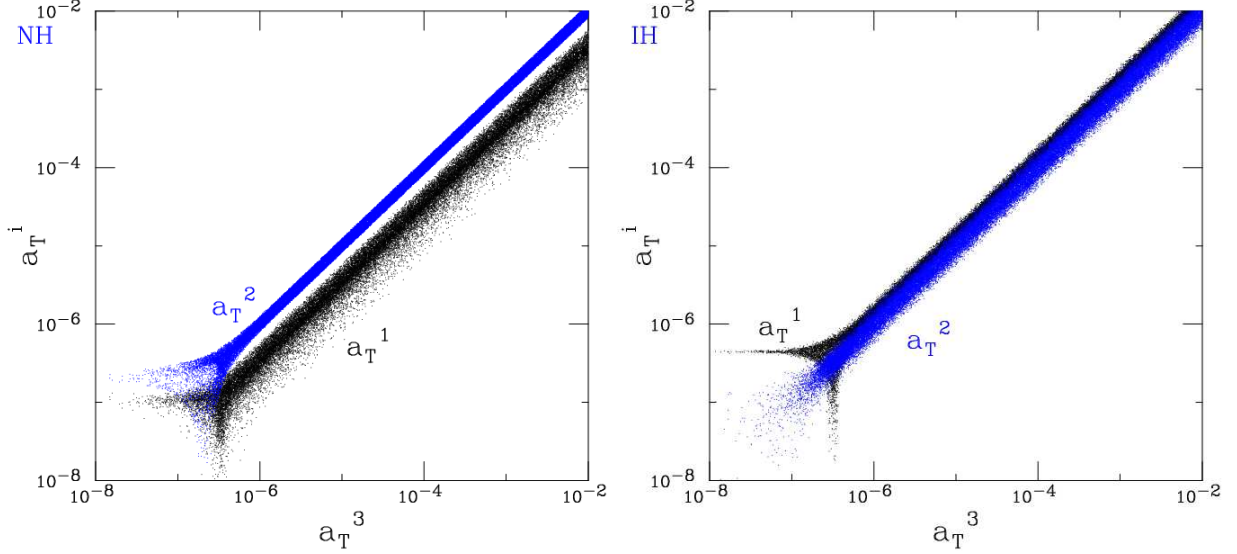


FIG. 2: Correlations between a_T^i 's for NH (left) and IH (right). $\Phi = 0$.

approximately factorize into a form independent of $\text{Re}(z)$

$$y_T^{i*} \propto \begin{cases} e^{\text{Im}(z)} \left((\Delta m_S^2)^{1/4} U_{i2} + i (\Delta m_A^2)^{1/4} U_{i3} \right), & \text{(NH)}, \\ e^{\text{Im}(z)} (\Delta m_A^2)^{1/4} (U_{i1} + i U_{i2}), & \text{(IH)}. \end{cases} \quad (17)$$

(c). We see the important correlations: due to the large mixing between $\mu - \tau$ from the atmospheric neutrino observation, the generic prediction is

$$a_T^1 < a_T^2 \approx a_T^3 \quad \text{for NH}, \quad (18)$$

$$a_T^1 > a_T^2 \approx a_T^3 \quad \text{for IH}. \quad (19)$$

(d). For $|z| \lesssim \mathcal{O}(1)$, the situation is less clear because of the dependence on $\text{Re}(z)$. The same feature is presented differently in Fig. 2 for $a_T^{1,2}$ versus a_T^3 . The band structure is due to the experimental uncertainties for the input parameters of the neutrino masses and mixing angles.

Including the Majorana phase Φ as an additional unknown parameter greatly increases the spread of a_T range as seen in Figs. 3 and 4. Although the generic features of Eqs. (18) and (19) should still remain, the prediction is less sharp due to the dilution of the phase parameters.

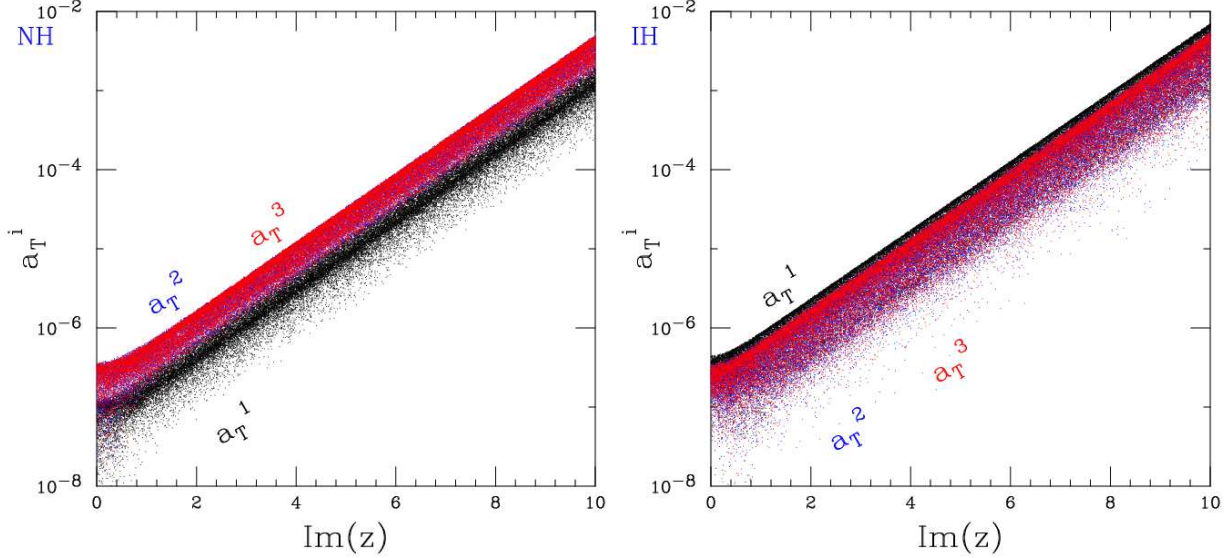


FIG. 3: a_T^i versus $\text{Im}(z)$ for NH (left) and IH (right). $\Phi \in [-\pi/2, \pi/2]$.

IV. DECAYS OF T

For the leptonic triplet in our model, there are a number of decay channels as well as rich new physics to explore.

A. $T \rightarrow W, Z, h + \text{light lepton}$

If kinematically accessible, the predominant decay modes of the triplet leptons are to a gauge boson (or a Higgs boson) plus a SM lepton [22], whose coupling strength is dictated by the neutral Dirac Yukawa couplings. The expressions are given in Appendix B. The partial width for each mode is proportional to the mass M_T . From Eq. (B8) one sees that the decays of T^0 , just like a heavy Majorana neutrino, violate lepton number by two units. Because of the firm prediction for the leptonic triplets to be light near the TeV scale, it opens up the possibility to observe these Majorana states at hadron colliders via this fairly background-free signature as first discussed in [13]. These results are consistent with the decay formula of the gauge boson modes, in accordance with the Goldstone boson equivalence theorem when $M_T \gg m_Z, m_h$.

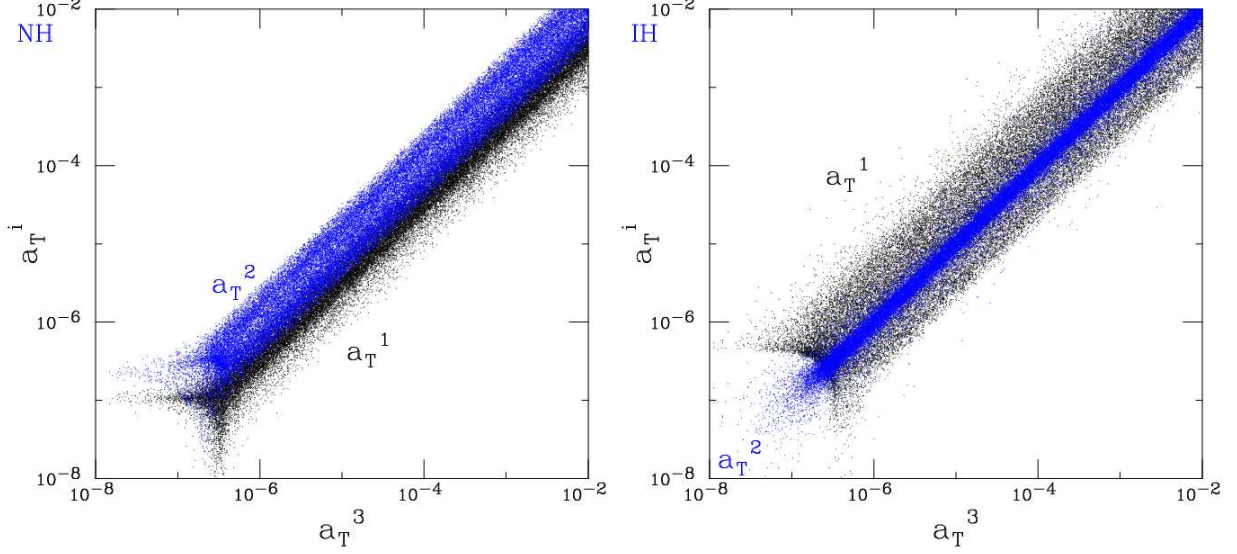


FIG. 4: Correlations between a_T^i 's for NH (left) and IH (right). $\Phi \in [-\pi/2, \pi/2]$.

B. $T^\pm \rightarrow T^0 \pi^\pm$

At the leading order, the heavy lepton triplet is mass-degenerate at M_T . Electroweak radiative corrections at one loop lift the degeneracy by a shift

$$\Delta M_T \equiv m_{T^+} - m_{T^0} = \frac{\alpha_2 m_W^2}{2\pi M_T} \left[f\left(\frac{M_T}{m_Z}\right) - f\left(\frac{M_T}{m_W}\right) \right], \quad (20)$$

$$f(y) = \frac{1}{4y^2} \log y^2 - \left(1 + \frac{1}{2y^2}\right) \sqrt{4y^2 - 1} \arctan \sqrt{4y^2 - 1}, \quad (21)$$

which gives $\Delta M_T \approx 160$ MeV with 10% accuracy in the whole range $100 \text{ GeV} \leq M_T \leq \infty$.

Given the rather small mass difference, the leading kinematically allowed decay mode is $T^\pm \rightarrow T^0 \pi^\pm$ with the decay width [35]

$$\Gamma_{\Delta M_T} = \frac{2G_F^2}{\pi} \cos^2 \theta_c f_\pi^2 \Delta M_T^3 \sqrt{1 - \frac{m_\pi^2}{\Delta M_T^2}}. \quad (22)$$

The corresponding lifetime is estimated to be $\mathcal{O}(10^{-10})$ sec ≈ 10 cm or more (with $f_\pi = 130$ MeV and $\cos^2 \theta_c \approx 0.95$). This decay mode is thus negligible in comparison with the $W^{\pm\nu}$ or Zl^\pm decay channels considered in the previous subsection (see below for details).

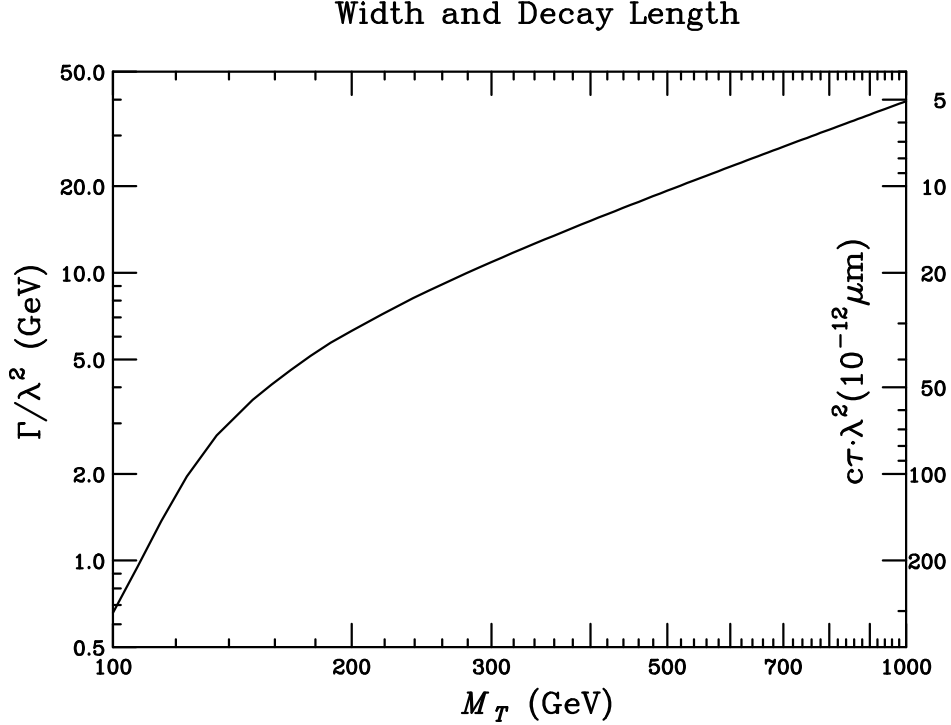


FIG. 5: Total widths (left axis) and proper decay lengths (right axis) of T^\pm/T^0 as functions of its mass.

C. Total widths and decay lengths

The total triplet decay width is given by the simple sum over the contributing channels

$$\Gamma_T = \frac{M_T}{32\pi} \left(\sum_k |y_T^k|^2 \right) \left[2f_1 \left(\frac{m_W}{M_T} \right) + f_1 \left(\frac{m_Z}{M_T} \right) + f_0 \left(\frac{m_h}{M_T} \right) \right] + \Gamma_{\Delta M_T}, \quad (23)$$

$$f_n(x) = (1 - x^2)^2 (1 + 2nx^2) \Theta(1 - x). \quad (24)$$

Given the couplings in our theory, the total width scales roughly linearly with the mass, particularly above the W , Z , and h thresholds:

$$\Gamma_T \approx 0.04\lambda^2 M_T, \quad \lambda^2 \equiv \sum_k |y_T^k|^2, \quad (25)$$

and the proper decay length

$$\tau_T = \frac{1}{\Gamma_T} \approx \frac{25}{\lambda^2 M_T} \approx \frac{1}{10^{13}\lambda^2} \left(\frac{100 \text{ GeV}}{M_T} \right) 0.5 \text{ mm} \quad (26)$$

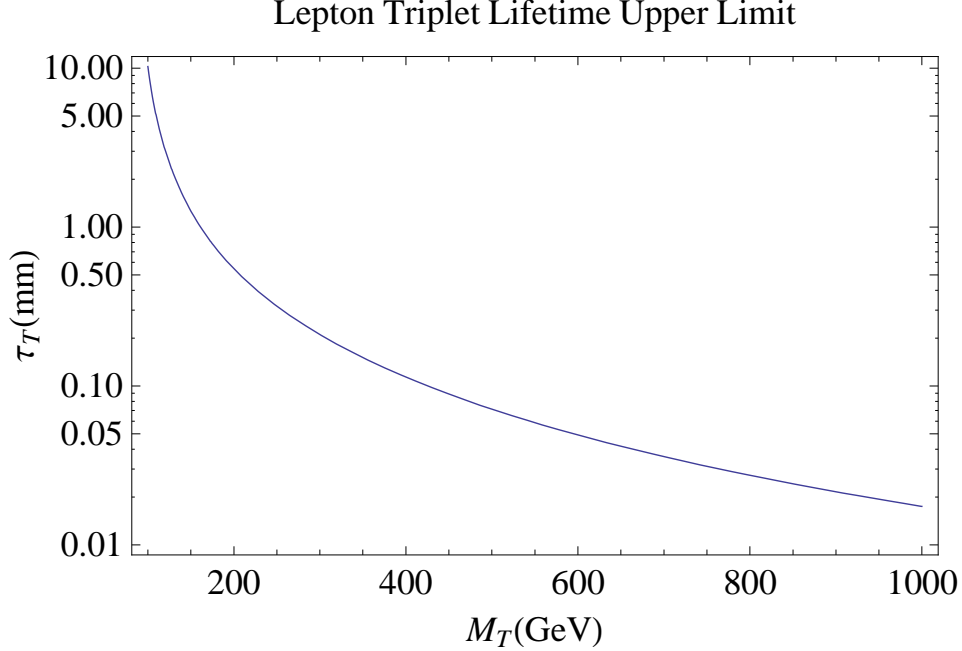


FIG. 6: The upper limit on the triplet lifetime as a function of its mass for $m_h = 120$ GeV.

On the other hand, making the connection to the neutrino masses as in Eq. (9), we have the lower bound in complete generality

$$\lambda^2 = \sum_k |y_T^k|^2 \geq \begin{cases} \frac{M_T}{v^2} \sqrt{\Delta m_S^2}, & \text{NH,} \\ \frac{M_T}{v^2} \sqrt{\Delta m_A^2}, & \text{IH,} \end{cases} \quad (27)$$

where in the IH case we approximated $\Delta m_A^2 - \Delta m_S^2 \approx \Delta m_A^2$. Using all the above we get an upper bound for the triplet lifetime (assuming for the moment that $\Gamma_{\Delta M_T}$ can be neglected)

$$\tau_T \leq \frac{32\pi}{\sqrt{\Delta m_X^2}} \left(\frac{v}{M_T} \right)^2 \frac{1}{2f_1(m_W/M_T) + f_1(m_Z/M_T) + f_0(m_h/M_T)} \quad (28)$$

with $X = S$ for NH and $X = A$ for IH. Taking the values of the neutrino masses as in Eq. (7) and the Higgs mass $m_h = 120$ GeV, one can easily calculate the upper limit for the triplet lifetime as a function of its mass. The limit in the NH case is shown on Fig. 6. For $M_T \gtrsim 200$ GeV (enough to saturate $f_n \rightarrow 1$) the upper lifetime limit can be approximated by

$$\tau_T \lesssim \left(\frac{200 \text{ GeV}}{M_T} \right)^2 0.5 \text{ mm} \quad (29)$$

In the IH case one has to divide the lifetimes by $\sqrt{\Delta m_A^2/\Delta m_S^2} \approx 5.6$. So in no case the decay $T^\pm \rightarrow T^0 \pi^\pm$ could be relevant [22]. This is different compared to the rank three

neutrino mass case considered in [15], where the lightest triplet decay can have arbitrarily small Yukawa couplings with the light leptons. In that limiting case the charged triplet decays to the neutral one and a pion in approximate 10 cm, while the neutral one does not have any upper limit, see also [35].

This leads us to conclude that the heavy leptons produced at the LHC experiments would decay inside the detector, possibly leaving displaced secondary vertices, but not appearing as stable particles. At least for small enough triplet mass the total lifetime could be measured directly. But even if not the total lifetime, the branching fractions into different final lepton states could be determined if not too small. This we discuss in the next subsection.

D. Branching fractions

Decay branching fractions of T to the three main decay channels involving W , Z and h are plotted in Fig. 7. Behavior in the low M_T region is dominated by threshold suppression. For sufficiently large M_T , these branching fractions approach their asymptotic values of $1/2$, $1/4$ and $1/4$, respectively. Due to the importance of charged leptons in the final state, we define the normalized branching fraction to a given charged lepton e_i ($e_i = e, \mu, \tau$ for $i = 1, 2, 3$), counted for the same final state gauge boson as

$$\text{NBR}_i \equiv \frac{\text{BR}(Ve_i)}{\sum_k \text{BR}(Ve_k)} = \frac{|y_T^i|^2}{\sum_k |y_T^k|^2}. \quad (30)$$

This quantity is universal for $V = W, Z, h$, and reflects the flavor structure of the final state leptons that is governed by the neutrino mass and mixing parameters. The $\text{Im}(z)$ dependence of NBR_i and their correlations are shown in Figs. 8, and 9, when ignoring the Majorana phase.

In most of the parameter space of NH (left panels), i.e. for $\text{Im}(z) > 1$, the normalized branching fraction for either $V\mu$ or $V\tau$ is about 0.35 to 0.55 and the normalized Ve branching is less than 0.1. We thus have the prediction

$$\text{BR}(V\mu) \approx \text{BR}(V\tau) \gg \text{BR}(Ve), \quad (31)$$

For the case of IH (right panels), we can establish similarly the rough order of branchings and the combinations.

$$\text{BR}(V\mu) \approx \text{BR}(V\tau) < \text{BR}(Ve), \quad (32)$$

Lepton Triplet Branching Fraction

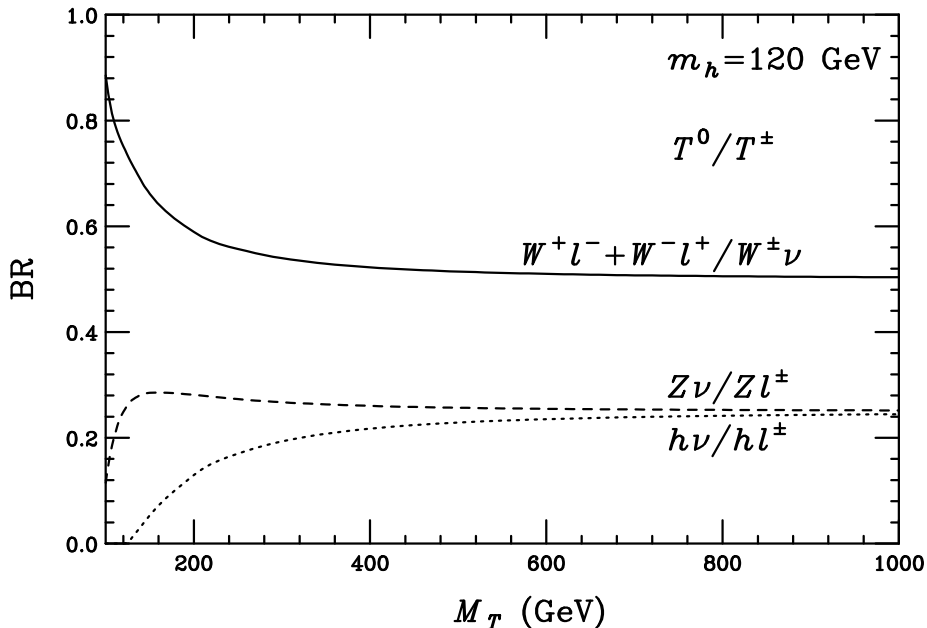


FIG. 7: Branching fractions of T^0/T^\pm as a function of its mass. A sum over lepton final states has been assumed.

Sizable Majorana phases may dilute the flavor correlations. The dependence of the flavor branchings on Majorana phases is shown in Fig. 10 for $\text{Im}(z) \geq 2$. The largest variations occur near $\Phi \approx \pm\pi/2$. It is important to note that (for $\text{Im}(z) \geq 2$):

- For NH, $\text{BR}(V\mu)$ is down (up) and $\text{BR}(V\tau)$ is up (down) by an approximate factor of two for $\Phi \approx \pi/2$ ($-\pi/2$) with respect to $\Phi = 0$, while $\text{BR}(Ve)$ is independent of the phase;
- For IH, $\text{BR}(V\mu) \approx \text{BR}(V\tau)$ in the whole Φ range and are highly suppressed at $\Phi \approx \pi/2$, where $\text{BR}(Ve)$ is up by a factor of two with respect to $\Phi = 0$.

We remind the reader again that one neutrino is massless in this set-up, a direct consequence of the underlying SU(5) symmetry.

For smaller $\text{Im}(z)$, the branching fraction dependence on Φ gets smeared up, as shown in Fig. 11 for $\text{Im}(z) = 1$. Instead, they have a clearer dependence on the real part of z , $\text{Re}(z)$, another phase with periodic behavior, as seen in Figs. 12 and 13 for $\text{Im}(z) = 0.5$ and 0, respectively. The reader should keep in mind that for large enough values of $\text{Im}(z)$ the

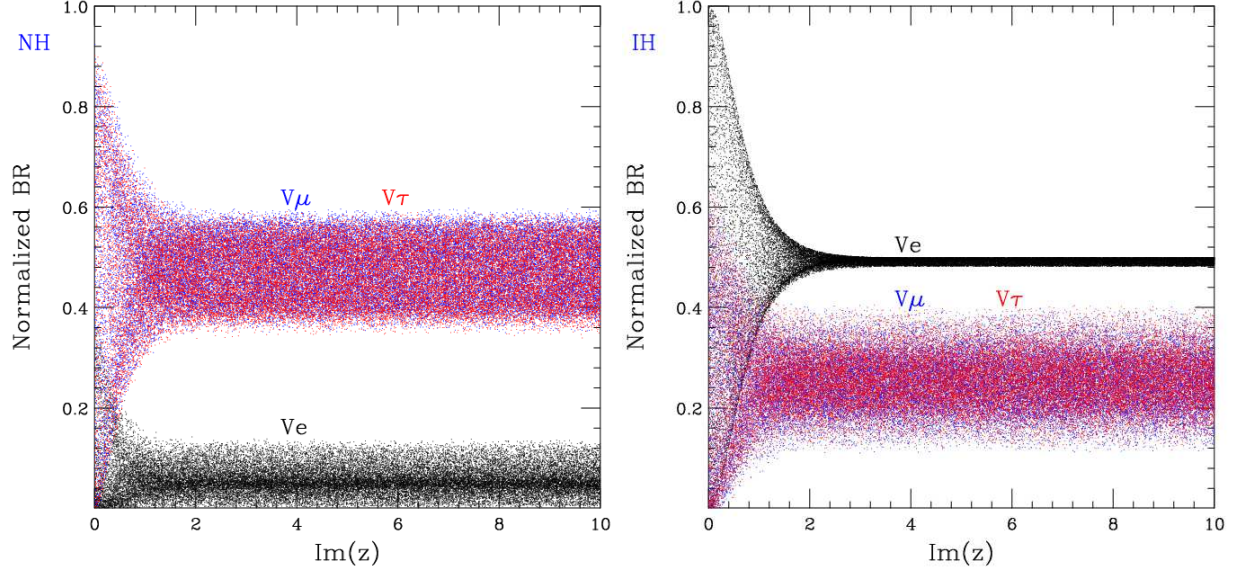


FIG. 8: Normalized branching of $T \rightarrow Ve_i$ (NBR_i) versus $\text{Im}(z)$ for NH (left) and IH (right); $\Phi = 0$.

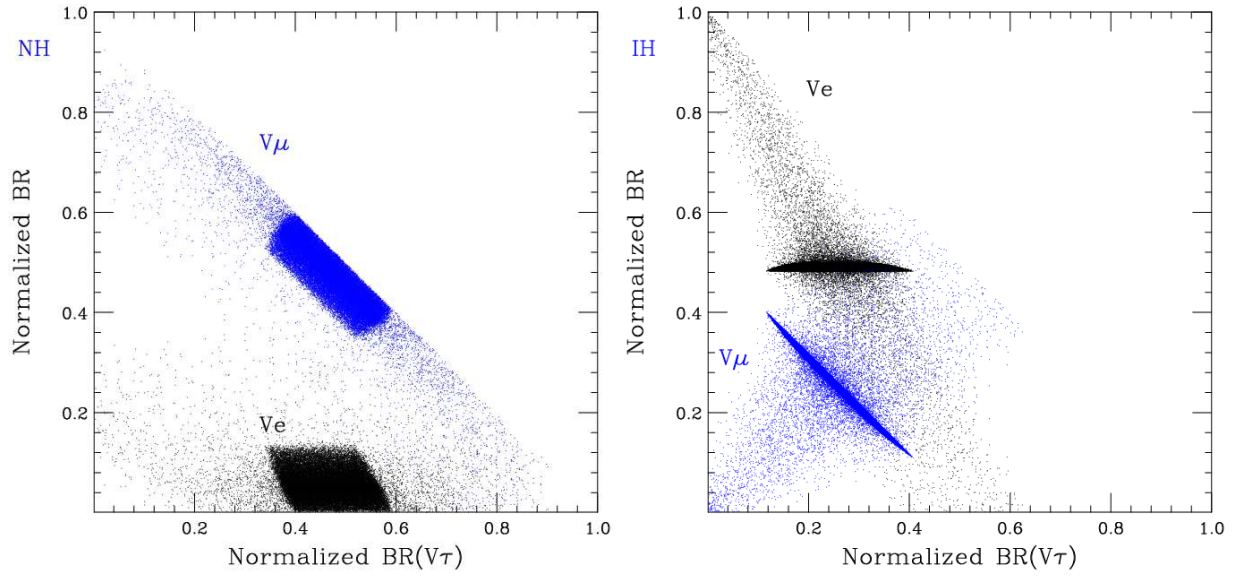


FIG. 9: Correlations between normalized branchings of $T \rightarrow Ve_i$ (NBR_i) for NH (left) and IH (right); $\Phi = 0$.

$\text{Re}(z)$ plays a much less significant role.

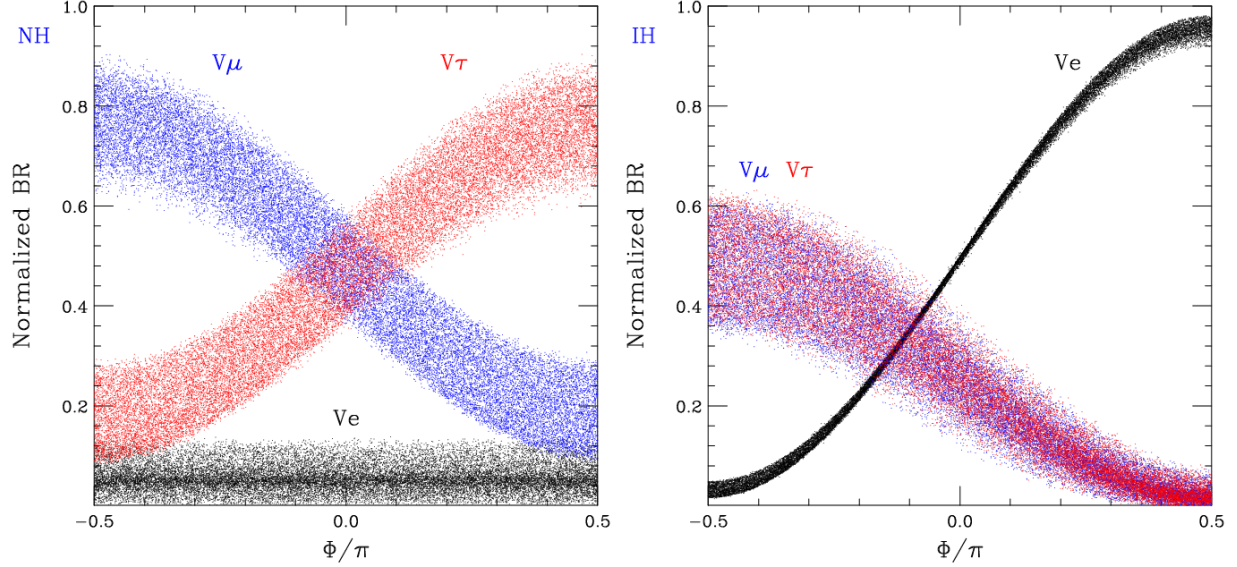


FIG. 10: Normalized branching versus Majorana phase for NH (left) and IH (right). $\text{Im}(z) \geq 2$.

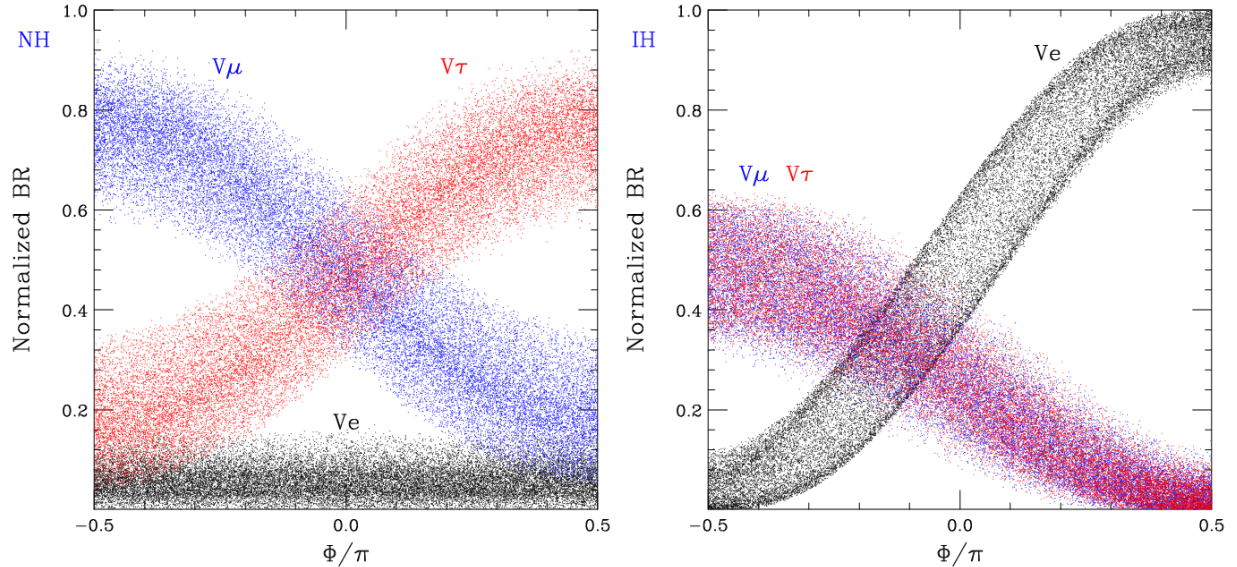


FIG. 11: Normalized branching versus Majorana phases for NH (left) and IH (right). $\text{Im}(z) = 1$.

E. Determining the leptonic mixing matrix

The message of the above discussion is that while one cannot make predictions yet for the various branching fractions, the collider signatures can shed light on the lepton mixing parameters. The theory in question has only two real parameters on top of the U_{PMNS} : $\text{Re}(z)$ and $\text{Im}(z)$. Since we can measure in principle two branching fractions and the total lifetime, one can get information on the yet unknown mixing angle θ_{13} and the Dirac and

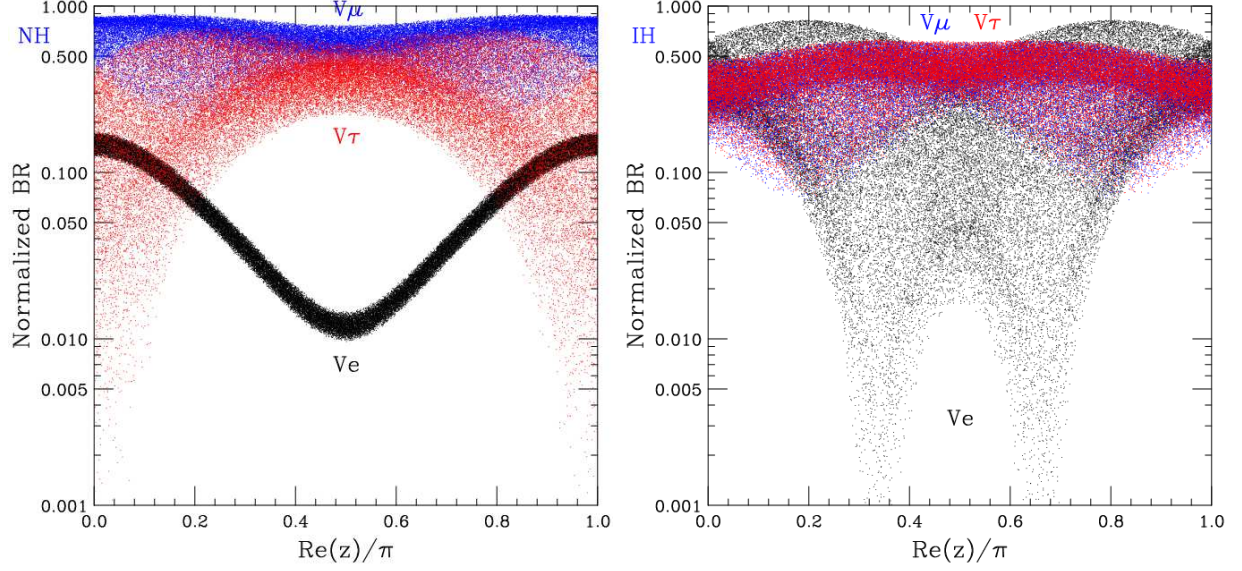


FIG. 12: Normalized branching versus $\text{Re}(z)$ for NH (left) and IH (right). $\text{Im}(z) = 0.5$ and $\Phi \in [-\pi/2, \pi/2]$.

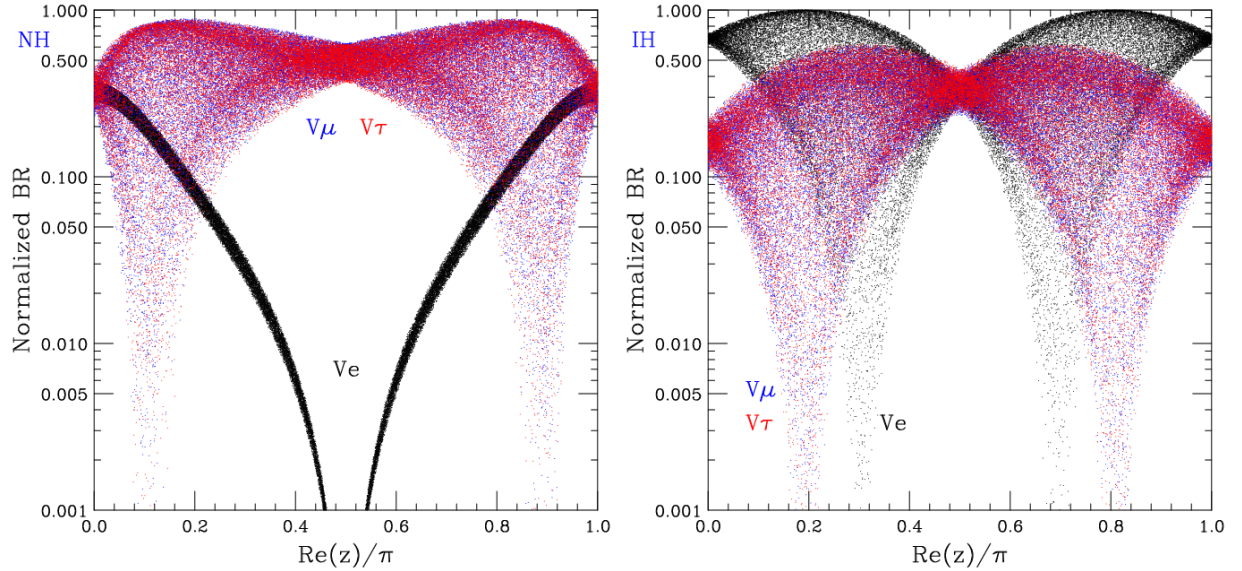


FIG. 13: Normalized branching versus $\text{Re}(z)$ for NH (left) and IH (right). $\text{Im}(z) = 0$ and $\Phi \in [-\pi/2, \pi/2]$.

Majorana phases δ and ϕ .

There is a good hope to probe θ_{13} in the near future through neutrino oscillation experiments. The large value of θ_{13} (close to the current experimental upper limit $\sin \theta_{13} \approx 0.18$) allows at least in principle for the determination of the Dirac phase δ . Together with the

observation of matter effects in oscillation, large θ_{13} allows also to distinguish the normal from the inverted hierarchy. On the other hand, for small values of θ_{13} , neutrino physics may not be sufficient to clear the above issues. Here the information from the LHC may be particularly handy. For this reason we highlight the small θ_{13} case. A few generic comments are warranted.

1) In this model it turns out that $\mu \rightarrow 3e$ dominates by large over $\mu \rightarrow e\gamma$ [30]. Simply the observation of $\mu \rightarrow e\gamma$ by the MEG experiment would eliminate this theory.

2) Since one neutrino is massless the neutrinoless double beta decay can play a clear role in distinguishing the normal from the inverted hierarchy. In particular, its observation in the next generation of experiments would rule out the normal hierarchy, as shown in Fig. 8.5 of [36] (see the far left limit of the far right plot).

3) The observation of $\mu \rightarrow 3e$ would imply large Yukawa couplings, which would in turn imply large $\text{Im}(z)$. In this limiting case the triplet lifetime would be too small to be measured. For normal hierarchy there is a clear prediction of less than 10% triplet normalized branching into electrons. So the final state with two electrons represents less than 1% of the total two charged lepton final states in this case.

For negligible θ_{13} (that we set to zero), in both NH and IH cases clear predictions emerge. In the case of IH one finds [22]

$$\frac{\text{NBR}_\tau}{\text{NBR}_\mu} = \tan^2 \theta_{23} \quad (33)$$

In the opposite case of NH the electron NBR and the total lifetime are functions of $\text{Re}[z]$ and $\text{Im}[z]$ only, which can thus be determined. The lifetime and the electron NBR cannot take arbitrary values, but are restricted, as can be seen from Fig. 14. The muonic NBR can then be used for the determination of the Majorana phase Φ , since the Dirac phase δ disappears in this case.

One could go on and on, but at this point it is not so useful due to the poor knowledge of the leptonic mixing matrix. As time goes on and knowledge of U_{PMNS} grows, there will be ample opportunity to return to these issues.

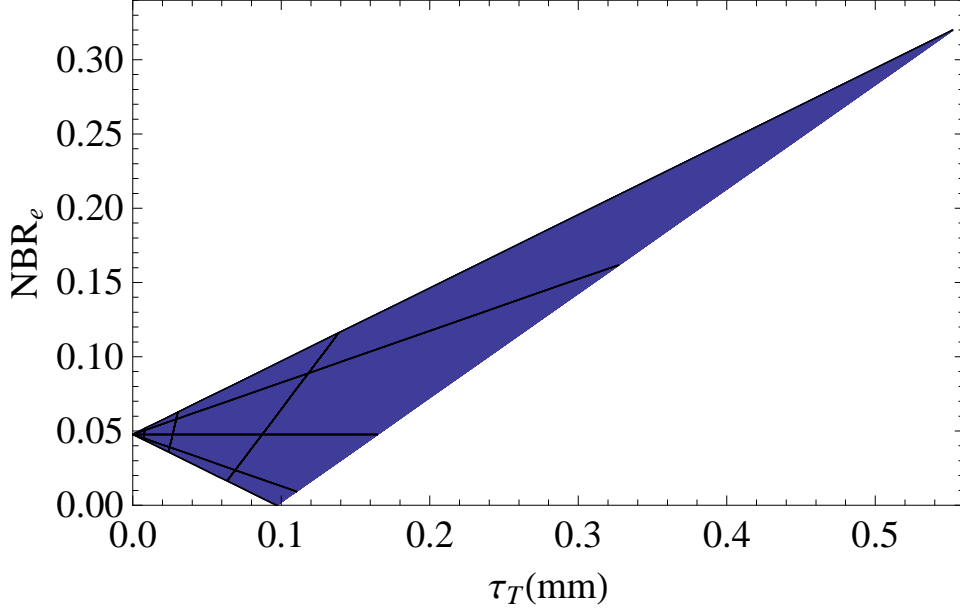


FIG. 14: The allowed values of the triplet lifetime and the electron normalized branching fraction in the NH case with $\theta_{13} = 0$, $M_T = 200$ GeV.

V. HEAVY LEPTON SIGNALS AT HADRON COLLIDERS

Based on the model discussed in section II, the leading production of the heavy triplet leptons at a hadron collider is via the Drell-Yan type processes

$$q\bar{q}' \rightarrow W^{*\pm} \rightarrow T^\pm T^0, \quad q\bar{q}' \rightarrow W^{*\pm} \rightarrow T^0 \ell^\pm, \quad (34)$$

$$q\bar{q} \rightarrow \gamma^*, Z^* \rightarrow T^+ T^-, \quad q\bar{q} \rightarrow Z^* \rightarrow T^\pm \ell^\mp. \quad (35)$$

Note that there is no tree-level process for $T^0 \bar{T}^0$ production. In our numerical analysis, we use the CTEQ6L1 parton distribution function [37] with factorization scale $Q = \sqrt{s}/2$, where s is the intermediate gauge boson four-momentum squared (or the parton-level CM energy squared).

A. Total cross sections

There are two main mechanisms to produce the heavy leptons in hadronic collisions: pair production of $T\bar{T}$, and associated single production $T e_i$. The cross sections for heavy pair production are well predicted by the SM gauge interactions. Those for heavy-light associated production are governed by the Yukawa coupling y_T^i . In Fig. 15, we present the

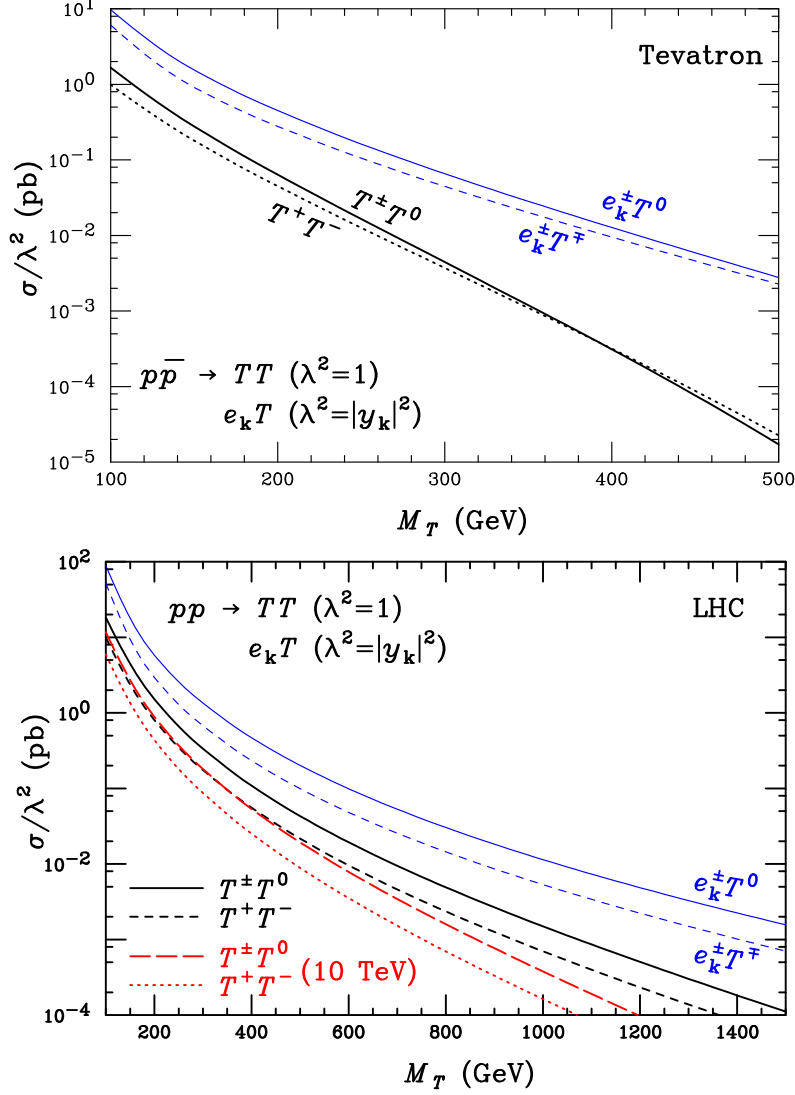


FIG. 15: Cross sections of single and pair productions of T^\pm/T^0 as a function of its mass, (a) at the Tevatron (1.96 TeV) and (b) at the LHC (14 TeV and 10 TeV). The scaling constant λ^2 is 1 for TT , and $|y_k|^2$ for $e_k T$.

total production cross sections for those processes versus the heavy lepton mass M_T , for (a) at the Tevatron (pp at $\sqrt{s} = 1.96$ TeV) and (b) at the LHC (pp at $\sqrt{s} = 14$ TeV and 10 TeV). To view the generic feature, we have pulled out the effective couplings λ^2 in the plots, which is normalized to unity for the pair production, and to the Yukawa coupling squared for the single production.

Given the consideration of Eq. (16) that leads to an upper bound on the Yukawa couplings of $|y_k|^2 < \mathcal{O}(10^{-3})$, we expect the single production to be much smaller than the pair

production of the heavy triplet via gauge interactions. Thus the potential signal observation at hadron colliders can be significantly enhanced over the case of Type I seesaw [38, 39], where the only weak signal comes from the $T^0 e_i$ type due to mass mixing. Generically, the charged current process of $T^\pm T^0$ production has a larger cross section than that of the neutral current for $T^+ T^-$ at the parton level. This leads to the larger cross section rate by about a factor of 2 at the LHC as seen in Fig. 15(b) by the solid and short-dashed curves, while they are about equal at the Tevatron due to the compensation from the larger valence quark luminosity $w\bar{u}$, $d\bar{d}$ for the neutral current. One sees that the cross section rate of the pair production can reach the order of 20 fb for $M_T \sim 250$ GeV at the Tevatron, and the order of 2 fb for $M_T \sim 1000$ GeV at the LHC. The cross sections at a 10 TeV LHC will drop to 60% – 50% at $M_T = 200 - 400$ GeV, and to 25% at $M_T = 1$ TeV, as given by the long-dashed and dotted curves in Fig. 15(b). We note that the pair production of the triplets is the same as that of the winos in Supersymmetric theories when we ignore the other superpartners [40]. Our results are in accord with this case.

B. Final states from the pair production of $T\bar{T}$

We focus on the pair production of the heavy triplets. The possible combinations of decay channels of pair-produced T 's are listed in Table. I, where ℓ denotes the observable charged lepton flavors e , μ and τ .

	$T^- \rightarrow \nu W^-$	$T^- \rightarrow \ell^- Z$	$T^- \rightarrow \ell^- h$
$T^0 \rightarrow \nu h$	$\nu\nu W^- h$	$\nu\ell^- Z h$	$\nu\ell^- h h$
$T^0 \rightarrow \nu Z$	$\nu\nu W^- Z$	$\nu\ell^- Z Z$	$\nu\ell^- Z h$
$T^0 \rightarrow \ell^- W^+$	$\nu\ell^- W^- W^+$	$\ell^- \ell^- W^+ Z$	$\ell^- \ell^- W^+ h$
$T^0 \rightarrow \ell^+ W^-$	$\nu\ell^+ W^- W^-$	$\ell^+ \ell^- W^- Z$	$\ell^+ \ell^- W^- h$
$T^+ \rightarrow \nu W^+$	$\nu\nu W^- W^+$	$\nu\ell^- W^+ Z$	$\nu\ell^- W^+ h$
$T^+ \rightarrow \ell^+ Z$	$\nu\ell^+ W^- Z$	$\ell^+ \ell^- Z Z$	$\ell^+ \ell^- Z h$
$T^+ \rightarrow \ell^+ h$	$\nu\ell^+ W^- h$	$\ell^+ \ell^- Z h$	$\ell^+ \ell^- h h$

TABLE I: Triplet pair decay channels to the SM particles. $\ell = e, \mu, \tau$.

We are set to search for the heavy leptons and to test the seesaw mechanism. We wish

to unambiguously identify the Majorana nature of T^0 . We are thus left with the unique channels with lepton number violation

$$T^0 T^\pm \rightarrow (\ell^\pm W^\mp)(\ell^\pm Z/h), \text{ or } \ell^\pm \ell^\pm W^\mp Z/h \quad (36)$$

with $\ell = e, \mu, \tau$, which violate lepton number by two units $\Delta L = 2$. We must require the hadronic decay modes of W, Z and h in order to manifestly preserve the unique feature of the lepton number violation. These particular final states are thus, without missing neutrinos,

$$\ell^\pm \ell^\pm j_1 j'_1 j_2 j'_2, \quad (37)$$

where $j_1 j'_1$ and $j_2 j'_2$ are from decays of W and Z/h , respectively. From the observational point of view, these final states have unique kinematical features and are quite clean. The lepton number violation has no genuine irreducible SM backgrounds.

It is particularly important to identify the lepton flavors for those final state processes. Given the predicted relations between the neutrino mass and oscillation parameters and the couplings, we tabulate the predicted leading channels of $\Delta L = 2$ processes along with the indicative ranges of their branching fractions in Table II, where the first two factors $(1/2)(1/4)$ come from the decay branching to a given boson $T^+ \rightarrow Z/h \ell^+$, $T^0 \rightarrow W^- \ell^+$ in Fig. 7, respectively, and the next factors are from the branching to specific flavor of charged leptons as in Figs. 8 and 9. We see a hierarchical order among the event rates of their flavor combinations.

$$\mu\mu, \mu\tau, \tau\tau \gg ee, \quad \text{for NH}, \quad (38)$$

$$\mu\mu, \mu\tau, \tau\tau < ee, \quad \text{for IH}. \quad (39)$$

The observation of these qualitative features should serve as direct test of our Type I + Type III Seesaw mechanism. For simplicity from the observational point of view, we will mainly consider e, μ final states, and only comment on the tau final state briefly. The final decay branching fraction of T^\pm, T^0, W^\pm, Z and h to the final state of Eq. (37) based on Table II is thus

$$BR = \begin{cases} \frac{1}{2} \frac{1}{4} \cdot (\frac{1}{2})^2 (70\%)^2 \approx \frac{1}{64}, & \text{only } \mu^\pm \mu^\pm \text{ for NH}, \\ \frac{1}{2} \frac{1}{4} \cdot (\frac{1}{2})^2 2 (70\%)^2 \approx \frac{1}{32}, & \text{both } e^\pm \text{ and } \mu^\pm \text{ for IH}. \end{cases} \quad (40)$$

Signal channels	Leading modes and BR	
	Normal Hierarchy	Inverted Hierarchy
$T^\pm T^0$		
$\Phi \approx 0$	$\mu^\pm \mu^\pm \quad \frac{1}{2} \frac{1}{4} \cdot (\frac{1}{2})^2$ $\tau^\pm \tau^\pm \quad \frac{1}{2} \frac{1}{4} \cdot (\frac{1}{2})^2$ $\mu^\pm \tau^\pm \quad \frac{1}{2} \frac{1}{4} \cdot (\frac{1}{2})^2 \cdot 2$	$e^\pm e^\pm \quad \frac{1}{2} \frac{1}{4} \cdot (\frac{1}{2})^2$ $e^\pm \mu^\pm \quad \frac{1}{2} \frac{1}{4} \cdot \frac{1}{2} \frac{1}{4} \cdot 2$ $e^\pm \tau^\pm \quad \frac{1}{2} \frac{1}{4} \cdot \frac{1}{2} \frac{1}{4} \cdot 2$ $\mu^\pm \mu^\pm \text{ (or } \tau^\pm \tau^\pm) \quad \frac{1}{2} \frac{1}{4} \cdot (\frac{1}{4})^2$
$\Phi \approx \pi/2$	$\mu : \times 1/2; \tau : \times 2$	$\text{BR}(Ve) \rightarrow 1$

TABLE II: Leading channels of $\Delta L = 2$ and the indicative ranges of their branching fractions, as discussed in the text for both cases of the NH and IH. Another factor of $(70\%)^2$ should be included to count for the 4-jet final state decays from W, Z and approximately from h as well.

C. Tevatron

We first explore the signal observability at the Tevatron. We define the signal identification with two charged leptons and four jets

$$\begin{aligned}
p_T(\ell) > 18 \text{ GeV}, \quad |\eta_\ell| < 2; \quad p_T(j) > 15 \text{ GeV}, \quad |\eta_j| < 3; \\
\Delta R(jj) > 0.4, \quad \Delta R(j\ell) > 0.4, \quad \Delta R(\ell\ell) > 0.3,
\end{aligned} \tag{41}$$

where the particle separation is $\Delta R(\alpha\beta) \equiv \sqrt{(\Delta\phi_{\alpha\beta})^2 + (\Delta\eta_{\alpha\beta})^2}$ with $\Delta\phi$ and $\Delta\eta$ being the azimuthal angular separation and rapidity difference between two particles. We further choose to look for e, μ events only, and demand there be no significant missing transverse energy

$$\cancel{E}_T < 15 \text{ GeV}. \tag{42}$$

In our parton-level simulation, we smear the lepton (electron here) and jet energies with a Gaussian distribution according to

$$\frac{\delta E}{E} = \frac{a}{\sqrt{E/\text{GeV}}} \oplus b, \tag{43}$$

where $a_e = 13.5\%$, $b_e = 2\%$ and $a_j = 75\%$, $b_j = 3\%$ (\oplus denotes a sum in quadrature) [41].

In Fig. 16, we show the total cross section in units of fb, for $p\bar{p} \rightarrow T^\pm T^0$ production and their decays at the Tevatron energy $\sqrt{S} = 1.96 \text{ TeV}$ as a function of the heavy lepton

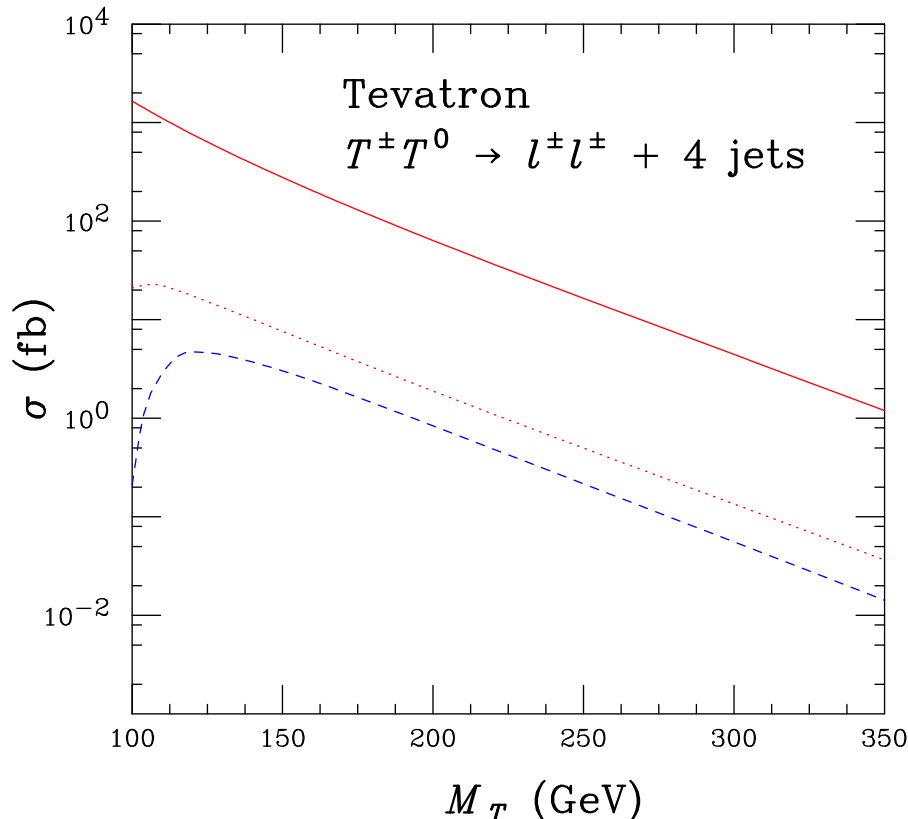


FIG. 16: Total cross section for $p\bar{p} \rightarrow T^\pm T^0$ production and decay at the Tevatron energy $\sqrt{S} = 1.96$ TeV as a function of the heavy lepton mass. The solid curve (top) is for the production rate of $T^+T^0 + T^-T^0$ before any decay or kinematical cuts. The dotted (middle) curve represents production cross section including appropriate branching fraction of Eq. (40), for the case of IH for illustration, with $\ell = e, \mu$ taken from the leading channels in Table II. The dashed (lower) curve shows variation of signal cross section after taking into account the cuts in Eqs. (41) and (42).

mass. The solid curve (top) is for the production rate of $T^+T^0 + T^-T^0$ before any decay or kinematical cuts. The dotted (middle) curve represents production cross section including appropriate branching fraction of Eq. (40) for the case of IH with $\ell = e, \mu$ taken from the leading channels in Table II. The dashed (lower) curve shows variation of signal cross section after taking into account all the kinematical cuts as in Eqs. (41) and (42). As a result of the cuts, the cross section is reduced by about a factor of 3. As mentioned above, these final states with lepton number violation have no genuine irreducible SM backgrounds. The other fake backgrounds from multiple W, Z production leading to the final state of Eq. (37)

the Tevatron energies are negligibly small. Assuming an integrated luminosity of 8 fb^{-1} is available in the near future, a 99% Confidence Level (CL) signal would require 5–7 events, that would lead to mass reach $M_T \sim 200 \text{ GeV}$ or higher. For the case of NH, the electron mode is absent while the tau mode shows up with a larger branching fraction, as a distinctive feature of this neutrino mass pattern.

Before ending this section, two remarks are in order. First, as argued in [42], the additional channels $e^\pm\tau^\pm$, $\mu^\pm\tau^\pm$ and $\tau^\pm\tau^\pm$ may be fully reconstructable kinematically. This will significantly enhance our signal observability, as well as the discrimination power for the NH and IH mass patterns as outlined in Table II. The τ identification would be particularly crucial if the effects of the CP phase are present. Further studies will be needed to incorporate the τ^\pm modes. Second, our results are based on parton level simulations although we have implemented the detector acceptance and smeared the energy and momenta. We realize that there will be additional detection efficiencies associated with the final state particle identification and construction. Even with high efficiencies of over 90% for each object [43], the complex final state of two leptons and four jets will result in about a factor of two reduction in rate. More realistic simulations are needed for further conclusions, that are beyond the scope of the current work.

D. LHC

The LHC signatures of the Type III seesaw and their background were already studied in the case of three lepton triplets [14, 15, 16, 17], while there is only one light triplet in our theoretical setting. Our results below are compatible with their findings whenever the comparison is possible.

At the LHC energies, we follow a similar approach for the signal search to the above. We select the events with two charged leptons and four jets by the following basic kinematical acceptance [44]

$$\begin{aligned}
 p_T(\ell) > 15 \text{ GeV}, \quad |\eta_\ell| < 2.5; \quad p_T(j) > 20 \text{ GeV}, \quad |\eta_j| < 3; \\
 \Delta R(jj) > 0.4, \quad \Delta R(j\ell) > 0.4, \quad \Delta R(\ell\ell) > 0.3.
 \end{aligned}
 \tag{44}$$

Once again, we look for clean e, μ events and demand there be no significant missing trans-

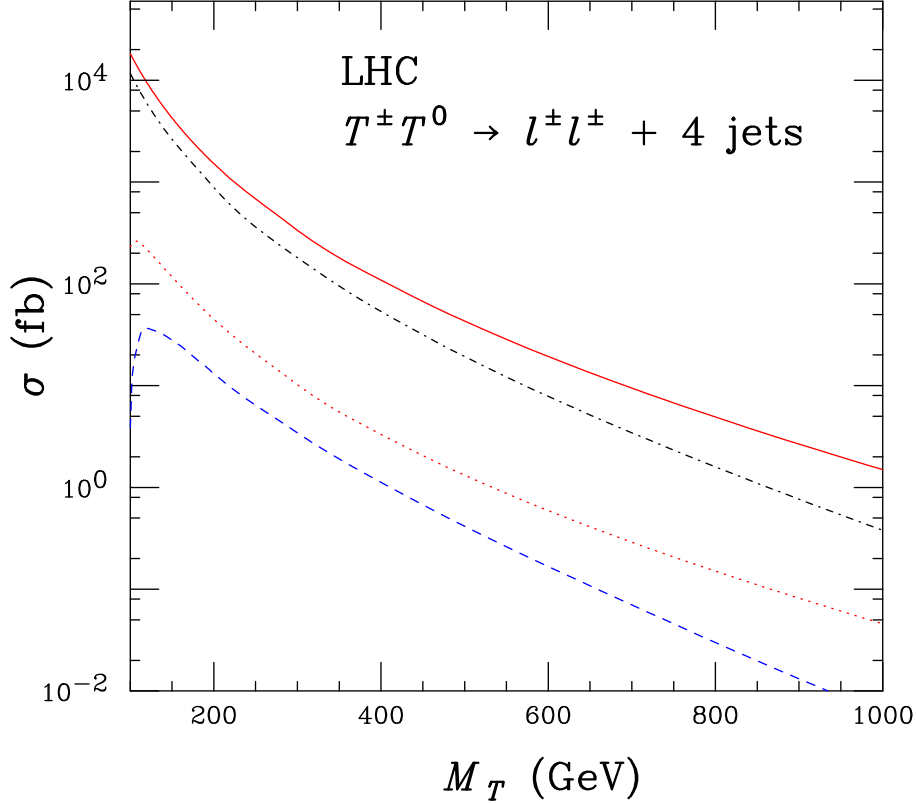


FIG. 17: Total cross section for $pp \rightarrow T^\pm T^0$ production and decay at the LHC energy at $\sqrt{S} = 14$ TeV as a function of the heavy lepton mass. The solid curve (top) is for the production rate of $T^+ T^0 + T^- T^0$ before any decay or kinematical cuts. The cross section at the 10 TeV LHC is also plotted (the curve right below) for comparison. The dotted (middle) curve represents production cross section including appropriate branching fraction of Eq. (40), for the case of IH for illustration, with $\ell = e, \mu$ taken from the leading channels in Table II. The dashed (lower) curve shows variation of signal cross section after taking into account the cuts in Eqs. (44– 47).

verse energy

$$\cancel{E}_T < 25 \text{ GeV}. \quad (45)$$

As for the energy smearing of the leptons and jets, we adopt the same form of Eq. (43), with the CMS parameterization $a_e = 5\%$, $b_e = 0.55\%$ and $a_j = 100\%$, $b_j = 5\%$. For simplicity, we did not separately smear the muon momenta by tracking, which would result in a better resolution at lower energies and become worse at higher energies, typically when $M_T \gtrsim 500$ GeV.

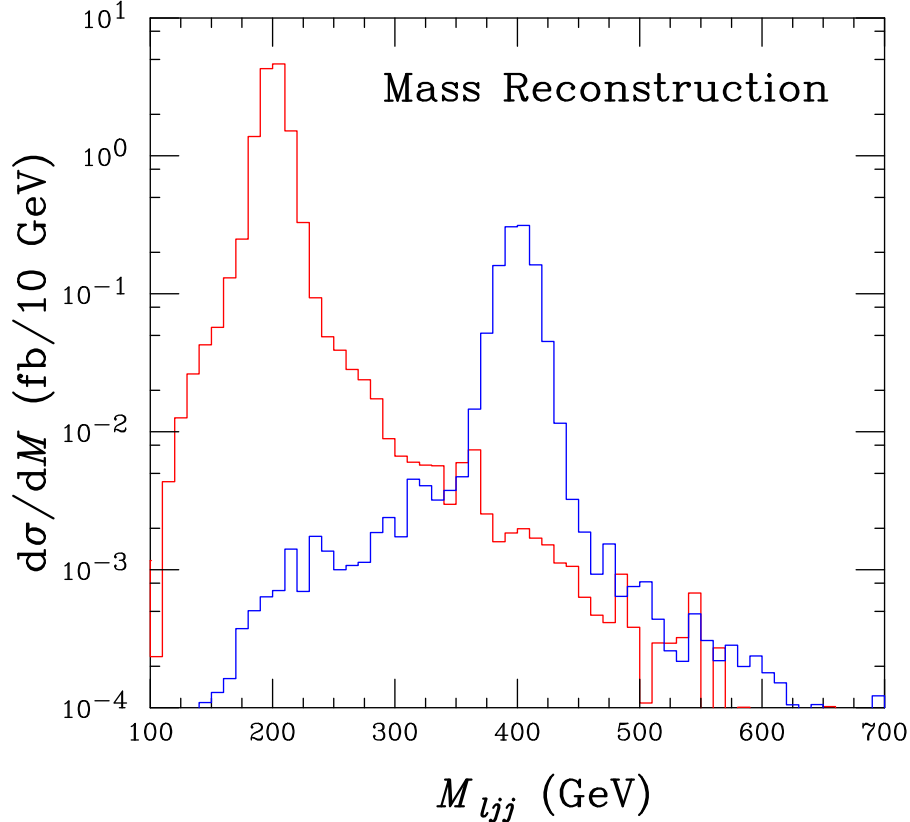


FIG. 18: Differential distribution of the reconstructed mass $M_{\ell jj}$ at the LHC for two representative values of heavy triplet lepton mass $M_T = 200, 400$ GeV. The energy bin size is 10 GeV.

In Fig. 17 we show the total cross section for $pp \rightarrow T^\pm T^0$ production at the LHC as a function of the heavy lepton mass. The solid curve (top) is for the production rate of $T^+T^0 + T^-T^0$ at $\sqrt{S} = 14$ TeV before any decay or kinematical cuts. The cross section at 10 TeV is also plotted (the dot-dashed curve right below). In comparison with LHC at 14 TeV, the rate is scaled down to 60% – 50% at $M_T = 200 - 400$ GeV, and to 25% at $M_T = 1$ TeV. The dotted (middle) curve represents production cross section including appropriate branching fraction of Eq. (40), for the case of IH for illustration, with $\ell = e, \mu$ taken from the leading channels in Table II. The dashed (lower) curve shows variation of signal cross section after taking into account all the kinematical cuts in Eqs. (44– 47). As a result of the cuts, similar to the discussions in the previous section, the cross section is reduced by about a factor of 4 for a modest lepton mass, but the reduction becomes more severe due to the fact that the decay products are more collimated for a much heavier lepton and that

σ (fb)	Basic	\cancel{E}_T	m_{jj} cut	$M_{\ell jj}$
Process	Cuts	< 25 GeV	$65 - 105$ GeV	200 ± 50 GeV
$T^\pm T^0, M_T = 200$ GeV	15.0	13.5	13.4	13.4
$T^\pm T^0, M_T = 400$ GeV	1.49	1.13	1.12	1.12 (400 ± 50 GeV)
$W^+W^+(W^-W^-)$ 4 jets	1.26 (0.51)	0.038 (0.024)	$7.6 (5.6) \times 10^{-3}$	$1.3 (1.0) \times 10^{-3}$
$W^+W^+W^-(W^-W^-W^+)$ 2 jets	3.2 (1.8)	0.14 (0.08)	0.087 (0.046)	0.032 (0.014)
Total backgrounds	6.8	0.28	0.15	0.048

TABLE III: Effects of the kinematical cuts on the production cross sections (in fb) at the LHC for the signal $pp \rightarrow T^\pm T^0 \rightarrow \ell^\pm \ell^\pm j_1 j_1' j_2 j_2' (\ell = e, \mu)$ as in the case of IH, and their leading SM backgrounds. We take $M_T = 200, 400$ GeV for illustration. The final state branching fractions have been included as given in Table II (IH). The background results in the last column are with a cut $M_{\ell jj} = 200 \pm 50$ GeV.

the faked missing energy increases.

To further purify the signal sample, we can consider constraining the di-jet mass $m(jj) \approx m_W, m_Z$ or m_h , where we will assume that the Higgs mass is already known. To break the combinatorial degeneracy of the three possible pairings for the four jets, we first pick the one that fits well with

$$65 \text{ GeV} < m(jj) < 105 \text{ GeV}, \quad \text{or} \quad 100 \text{ GeV} < m(jj) < 140 \text{ GeV for } h. \quad (46)$$

The most important feature of our signal events is the effective reconstruction of the heavy lepton mass from the final state leptons and jets $M_{T^\pm} \approx m(\ell jj)_1 \approx M_{T^0} \approx m(\ell jj)_2$. The complication again is the combinatorial, with two choices of pairing for $\ell_{1,2}$ and $(jj)_{1,2}$. The best reconstruction is the one which has the least difference between the two reconstructed invariant masses m_1 and m_2 and the best reconstructed heavy lepton mass is the corresponding mean value $M_{\ell jj} = (m_1 + m_2)/2$. In Fig. 18 we show the differential distribution of the reconstructed mass $M_{\ell jj}$ for two representative values of heavy lepton masses, 200 and 400 GeV. It is evident from the shape of the distribution and location of the peak that the reconstruction of the heavy lepton mass can be quite effective using the technique mentioned above. Since the physical width of the heavy lepton is very narrow, the broad distribution at the peak is largely due to the detector resolution of the leptons and jets. Moreover, we

do not expect formation of such a peak at those particular values from SM backgrounds. The background can at most contribute to a continuum distribution. We thus propose to examine a wide window for the reconstructed mass peak

$$M_T \pm 50 \text{ GeV}, \quad (47)$$

when estimating the signal statistical significance. In Fig. 17, the short dot-dashed (lower) curve shows variation of signal cross section after taking into account all cuts as discussed in the text. The signal efficiency for the cuts are as high as 25% for $M_T \approx 200 - 600 \text{ GeV}$.

Although there is no intrinsic SM background to the lepton-number violating processes, there are always some fake backgrounds that lead to some similar final states to our signal events. We have estimated the different contributions using Madgraph/Madevent [45]. The immediate background to the $\ell^\pm \ell^\pm 4j$ signal that comes in mind will be

$$W^\pm W^\pm + 4 \text{ QCD jets.}$$

This background with our basic acceptance cuts has a cross section of 1.8 fb. After the selective cuts for the mass reconstructions, it is reduced to a negligible level, about three orders of magnitude down. A larger background is from

$$W^\pm W^\pm W^\mp + 2 \text{ jets} \rightarrow W^\pm W^\pm + 4 \text{ jets},$$

in which about 90% of the events are actually from $t\bar{t}W^\pm \rightarrow W^\pm W^\pm b\bar{b} + 2 \text{ jets}$. With the appropriate branching fraction $BR(W \rightarrow l\nu)^2 BR(W \rightarrow jj) \approx 0.028$, the total cross section is about 15 fb and is reduced to about 5 fb with the basic acceptance cuts. After the selective cuts for the mass reconstructions, this background can be reduced by two orders of magnitude, to about 0.05 fb at $M_T = 200 \pm 50 \text{ GeV}$. It becomes negligible at a higher mass window.

Other backgrounds include $W^\pm W^\pm Z + 2 \text{ jets}$ and $W^\pm W^\pm VV$ ($V = W, Z$). These processes are rather small in production rate, typically less than 1 fb to begin with. We will not consider them further.

Another potentially large background is from the b decays that give a charged lepton. However, it is known that the stringent requirement of the lepton isolation would effectively separate the heavy quark backgrounds. Quantitatively, the suppression efficiency is difficult to estimate reliably and perhaps will be better understood once the real data become available.

In Table III, we show the incremental effect of different cuts on the signal cross section for two different values of heavy triplet lepton masses, 200 GeV and 400 GeV, respectively, along with the leading SM backgrounds. Again, the signal events are essentially background free after all of the kinematical reconstructions. To reach a 99% CL, the signal would require 5–7 events, that would lead to a mass reach $M_T \sim 450\text{--}480$ (700–740) GeV with an integrated luminosity of 10 (100) fb^{-1} .

As already noted in the previous section, we reiterate that the additional channels $e^\pm\tau^\pm$, $\mu^\pm\tau^\pm$ and $\tau^\pm\tau^\pm$ may be fully reconstructable kinematically [42]. This will significantly enhance our signal observability as well as the discriminating power between the NH and IH mass patterns. As seen in Table II, τ identification would be particularly crucial if the effects of the CP phase are present. On the other hand, we have not performed detailed detector simulations in our studies. Even with high reconstruction efficiencies of over 90% for each object [44], the complex final state of two leptons and four jets will result in about a factor of two reduction in rate. More realistic simulations are needed for further conclusions, which are beyond the scope of the current work.

E. The conspiracy problem: how to distinguish triplets from doublets

The main point of our paper is the search for a light fermionic triplet with $\Delta L = 2$ lepton number violating signatures such as same-sign dileptons plus jets without significant missing energy at the LHC. Although we have established the signal observability for the lepton number violating processes in a large region of the parameter space, it is important to ask if we can confirm the triplet nature of the signal that does not follow from other sources of different new physics in the leptonic sector. The existence of the charged heavy leptons could be from either a gauge doublet or triplet. Can the doublet of leptons leads to similar or, worse, same predictions? The answer is possibly yes. We explore the means to distinguish them both qualitatively and quantitatively. The extra doublet of leptons can be either a part of a chiral sequential fourth generation or a vector-like particle, that we discuss next in turn.

1. *Sequential fourth generation heavy leptons*

The immediate example would be the fourth family sequential heavy leptons. There are a number of features that will distinguish the fourth family case from the (three family) triplet case.

- 1 **The 4th family quarks:** In an anomaly-free formulation, there will be a new family of quarks. Due to the strong production, the new heavy quarks should be much easier to observe at the LHC up to a mass about 700 GeV [44] or higher.
- 2 **Gauge coupling strength in charged currents:** An obvious difference between the doublet and the triplet is their gauge couplings, as summarized in the Appendix. It turns out that the pair production cross section for a triplet is larger than that for a doublet by a factor of two. Although it would be non-trivial to determine the cross section normalization at the LHC for some processes with a complex final state, we are optimistic to assume that our channel is clean and the cross section can be determined with sufficient statistics when $M_T \sim 500$ GeV.
- 3 **Charged-neutral mass difference:** In the triplet model under consideration, there is a high degree of degeneracy of the triplet, $\Delta M_T \lesssim 160$ MeV. This is in great contrast to a sequential doublet model, where the lepton masses are not predicted. In fact, the fit to the electroweak oblique parameter ΔS indicates a preference for a significant mass splitting, on the order of 30 – 60 GeV, between the charged and the neutral leptons [46]. Due to this the dominant channel for the decay of the charged heavy lepton becomes a neutral one (N , a Majorana neutrino) plus an off-shell W . This means that the $E^\pm N$ production may lead to two same-sign leptons plus six jets (instead of four in the triplet case $T^\pm T^0$). For the same reason the $E^+ E^-$ production in the doublet case will even lead to lepton number violating signatures of $\ell^\pm \ell^\pm + 8$ jets. A word of caution is needed: it is not impossible that future studies find yet another possibility for extra sequential generation even with degenerate leptons. For this reason we study carefully the other distinguishable features at the international linear collider in the next section.
- 4 **Neutral current coupling:** The new feature of the doublet is that the neutral lepton couples to the Z boson, which distinguishes it crucially from the triplet, as summarized

in the Appendix. The production of a pair of neutral heavy leptons is absent in the triplet model, and is negligibly small for a gauge singlet N as well. Any clear signal for $N\bar{N}$ production would indicate a lepton doublet.

However, if the signal $N\bar{N}$ yields the final state $\ell^\pm\ell^\pm + 4$ jets, it would be difficult to tell them apart from the triplet signal as we discussed earlier, due to the fact that the W and Z in their hadronic decays are indistinguishable in the LHC environment. It is only hopeful through the four charged lepton mode with missing energy $\ell^+\ell^-\nu\ell^+\ell^-\bar{\nu}$. Such events will not have a resonant structure for $N \rightarrow \ell^\pm W^\mp, \nu Z$; while they will reveal the mass peak for $T^\pm \rightarrow \ell^\pm Z \rightarrow \ell^\pm\ell^+\ell^-$.

Let us remind the reader that in general there will be a non-negligible non-diagonal heavy-light leptonic coupling to Z . In the standard model the off diagonal lepton couplings to Z are suppressed by tiny neutrino masses and thus completely negligible. Since the fourth neutral lepton has to be heavy, it is easy to generate the above mentioned vertex through the GIM at one loop, even if the fourth generation mixes very little with the first three.

5 Chiral couplings: Perhaps the most conclusive test for the lepton doublet is to establish the charge forward-backward asymmetry, due to the chiral feature of their couplings. However, since we are unable to distinguish W and Z in their hadronic decay, we may have to rely on the pure leptonic decay of the Z , such as $T^+T^- \rightarrow \ell^+\ell^+\ell^-, \ell^-\ell^+\ell^-$, that would suffer from low statistics and the potential ambiguity in identifying the incoming quark direction. On the other hand, this type of measurements would be straightforward at an e^+e^- linear collider, as we will comment on later.

Obviously, there is no guarantee that either one of the above should be readily observable at the LHC. However, the confirmation of any of the above signatures would be nearly convincing to establish a triplet or a doublet model.

2. Vector-like heavy lepton doublet

Another prominent example would be a vector-like heavy lepton. The characteristic features discussed in points 2, 3 and 4 in the previous section are still valid. Let us elaborate

them.

- 1 **Gauge coupling strength:** As summarized in the Appendix, due to the stronger gauge coupling for the triplet. the pair production cross section for a triplet is larger than that for a doublet by about a factor of two.
- 2 **Charged-neutral mass difference:** The crucial new feature in this case is that one can not have the degeneracy and appreciable lepton number violation. The vector-like nature of the doublets L_L and L_R

$$L_{L,R} = \begin{pmatrix} N \\ E \end{pmatrix}_{L,R} \quad (48)$$

implies a gauge invariant mass term

$$- \mathcal{L}_{Dirac} = M_D \bar{L}_L L_R + h.c. = M_D (\bar{E} E + \bar{N} N) \quad (49)$$

where as usual $E \equiv E_L + E_R$ and in the same manner $N \equiv N_L + N_R$. At first glance there is a conspiracy because of the complete degeneracy between the charged and the neutral lepton, just as in the triplet case. However, as opposed to the triplet case, at this point the neutral lepton is a Dirac particle, which implies no lepton number violating signatures as the ones discussed throughout our paper.

Lepton number violation requires breaking the degeneracy through the Majorana masses

$$- \mathcal{L}_{Majorana} = \delta M_L N_L N_L + \delta M_R N_R N_R + h.c. . \quad (50)$$

These mass terms can simply emerge due to Weinberg-like dimension 5 operators and they will lead to lepton number violation proportional to $(\delta M_{L,R}/M_D)^2$. Clearly in order not to be too small, the degeneracy between E and N must be substantially broken through $\delta M_{L,R}$. This strongly broken degeneracy will surely discriminate between the triplet and vector-like doublet.

- 3 **Neutral current coupling:** Also, as in the case of sequential fourth generation heavy leptons, the neutral lepton N couples to the Z , so that the above discussion follows here as well.

VI. HEAVY LEPTONS AT A LINEAR COLLIDER

It has been demonstrated in Ref. [47] that physics at the LHC and the e^+e^- International Linear Collider (ILC) will be complementary to each other in many respects.

In this section we study the production of a pair of heavy leptons (E^\pm) at a linear collider. As discussed above, those heavy leptons can originate either from a triplet model with the Type III Seesaw mechanism, a sequential fourth generation leptons model, or a vector-like doublet model. In those three scenarios, the heavy leptons couple differently to the Z boson. For triplet fermions and vector-like leptons, the coupling to the Z boson are purely vectorial, while a sequential fourth generation lepton has also an axial coupling which will lead to a non vanishing forward-backward asymmetry as will demonstrate later. We summarize these couplings in Table IV of Appendix A.

At an e^+e^- collider, the only Feynman diagrams that contribute to a pair production of heavy leptons are the photon and Z boson s -channel exchange. The corresponding cross section formulae are given in Appendix B. The total cross sections for the three models under consideration are illustrated in Fig. 19, as a function of (a) the center-of-mass energy \sqrt{s} for $M_E = 200$ GeV (left panel) and (b) M_E for $\sqrt{s} = 1$ TeV (right panel). It is clear from the plots, that the sequential doublet and vector-like model gives a similar cross section while the triplet model give a cross section which is more than twice as large. The reason is that in the case of triplet model the purely vectorial coupling of $-2\cos^2\theta_W$ is much larger than the corresponding couplings for doublet and vector-like, as listed in Table IV.

As one can see from Fig. 19(a), the total cross section above the threshold can reach 700 fb for $\sqrt{s} = 500$ GeV and a triplet mass of 200 GeV. For an integrated luminosity of 500 fb^{-1} , this cross section would yield a couple of hundred thousand events before the detector acceptance. For center of mass energy around 1 TeV, the cross section for a triplet is still about 200 fb for masses in the range of 200–400 GeV.

The process for triplet or vector-like leptons with $Z\bar{E}E$ coupling purely vectorial ($a_E = 0$) has an angular distribution of the generic form

$$\frac{d\sigma}{d\cos\theta} \propto a(1 + \cos^2\theta) + b(1 - \cos^2\theta), \quad (51)$$

with θ the scattering angle between the e^- beam and E^+ . This angular distribution gives a vanishing forward backward asymmetry due to parity conservation. This would distinguish

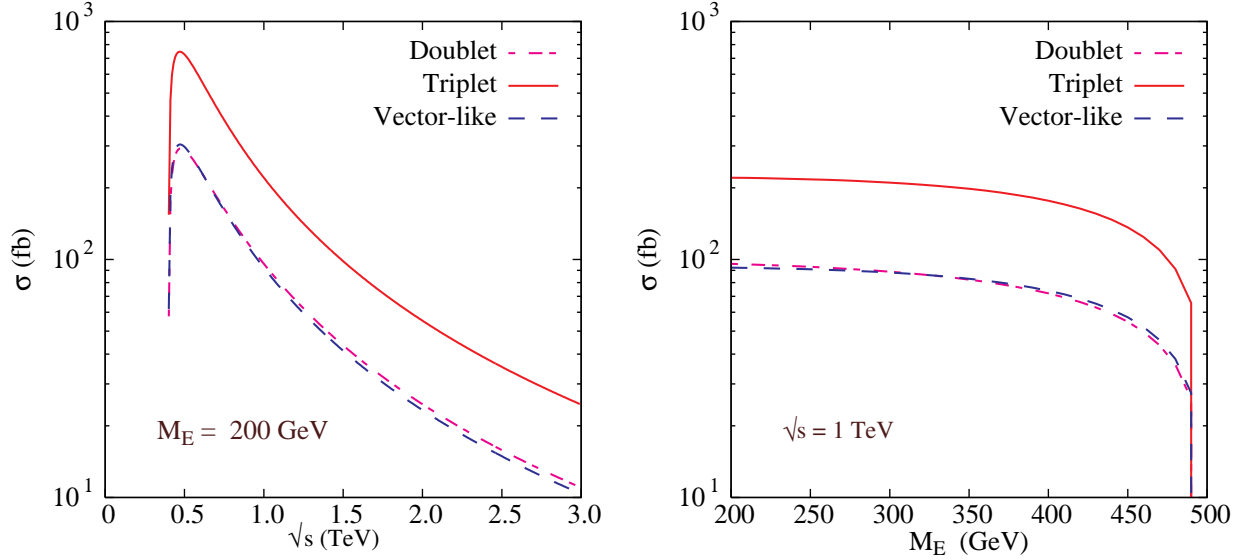


FIG. 19: $\sigma(e^+e^- \rightarrow E^+E^-)$ in units of fb as a function of center-of-mass energy \sqrt{s} with $M_E = 200$ GeV (left), and as a function of M_E with $\sqrt{s} = 1$ TeV for a triplet, a sequential fourth generation and vector-like doublet models.

between the triplet and a sequential leptonic doublet. In Fig. 20 we illustrate the angular distributions normalized to the total cross section for $M_E = 200$ GeV, $\sqrt{s} = 500$ GeV (solid curves) and $M_E = 300$ GeV, $\sqrt{s} = 1$ TeV (dotted curves). As expected from the above discussion, the angular distribution for the triplet and vector-like fermion is completely symmetric and would give vanishing forward-backward cross section. While in the case of sequential fourth generation leptons we get an asymmetric angular distribution which would give a forward-backward asymmetry of the order of 50% (70%) for $\sqrt{s} = 500$ GeV (1 TeV). Evidently, the asymmetry variables would be the most conclusive test of the chiral nature of the couplings. Even with a clear signal observation of heavy lepton production at the LHC, the fact that it is hard to determine the absolute cross section and to measure an asymmetry in an angular distribution makes an e^+e^- linear collider an ideal machine for detailed property studies.

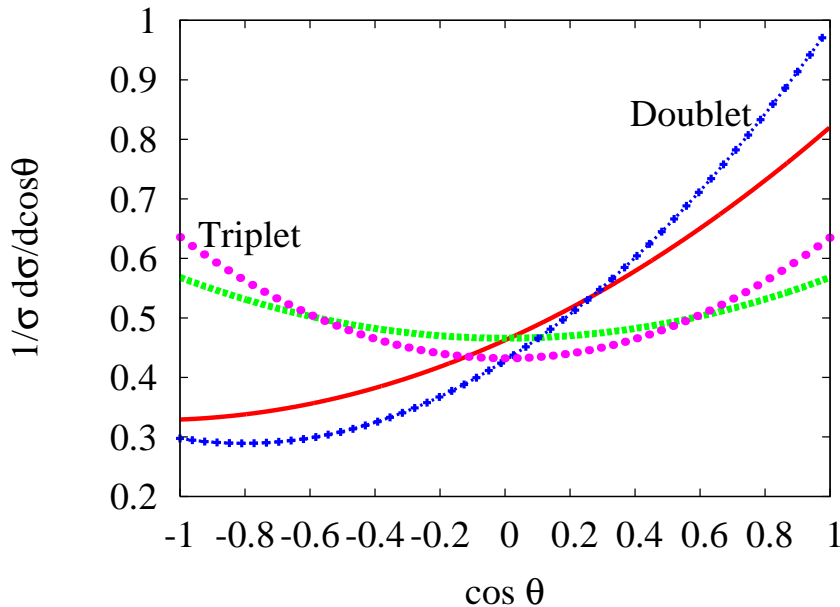


FIG. 20: Normalized angular distributions for a pair production of lepton doublet (forward) and triplet (central) with $M_E = 200$ GeV and $\sqrt{s} = 500$ GeV (solid curves) and $M_E = 300$ GeV and $\sqrt{s} = 1$ TeV (dotted curves).

VII. CONCLUSIONS

The minimal Georgi-Glashow SU(5) model is a remarkably predictive grand unified theory. It leads to massless neutrinos and it fails to unify the SM gauge couplings with the current accuracy from the electroweak precision measurements. In a sense the failure of the minimal theory may be for the best, for it predicted the desert, with no new physics beyond the electro-weak scale, all the way up to the M_{GUT} around 10^{16} GeV or so. Even if correct, it would leave us with nothing new to observe at the next generation of colliders such as the LHC, and we would have only indirect tests, albeit exciting, such as proton decay. The desert could have an oasis of supersymmetry, but its motivation is mainly inspired by the hierarchy issue and not a physical, phenomenological need. And, strictly speaking, the supersymmetry scale could be above the reach of LHC energies, leaving us with a mild hierarchy issue, far less dramatic than the original one of the doublet-triplet splitting.

Instead, one can ask what is the minimal extension that can give realistic neutrino masses and mixings and the unification of gauge couplings. It turns out that augmented by an adjoint fermion, it remains equally remarkably predictive but now in accord with the experi-

ment. In the popular seesaw language it is a hybrid of Type I and Type III and automatically predicts one massless neutrino. The Type III triplet fermion must lie below TeV and should be looked for at the LHC. Its decays probe the Yukawa couplings responsible for the neutrino mass matrix. It is noteworthy that the term predictive is used here in a narrow strict sense: no further assumption or principle has been used beyond the one of grand unification.

In summary, in the Georgi-Glashow SU(5) the desert was intimately related with the desire of massless neutrinos. Non vanishing neutrino masses lead a number of oasis in the desert, and mostly important offer new physics for the LHC. If anything, this can be viewed as an example of how a phenomenological motivation of neutrino masses and mixings can lead to new phenomena at the LHC, and provides a counter example to a prejudice that the seesaw mechanism in the context of grand unification needs new large scales. Just as right handed neutrinos of the Type I seesaw tend to lie close to M_{GUT} in SO(10), here the mass of the analogous SU(2) triplet fermion must lie below TeV.

In this paper we have offered an in-depth study of the collider signatures of this model at colliders such as the Tevatron, the LHC, and an e^+e^- linear collider. The smoking gun is the production of lepton number violating same-sign dileptons plus four jets without significant missing energy. Our analysis shows that for an integrated luminosity of 8 fb^{-1} , the Tevatron could probe the lepton triplet up to a mass 200 GeV. At the LHC with a luminosity of 10 (100) fb^{-1} , one may probe the triplet up to a mass 450 (700) GeV. We also provide some general remarks on how to distinguish the lepton triplet from other heavy leptonic states. As a complementary study in this regard, we present the results for cross sections and distributions at an e^+e^- linear collider for a few representative models.

Acknowledgment

We thank Ilja Doršner, Pavel Fileviez Perez, Srubabati Goswami, Michel Herquet, Anjan Joshipura, Borut Kerševan, Rajko Krivec, Miha Nemevšek, Kerim Suruliz and Enkhbat Tsedenbaljir for discussion and correspondence. A.A., D.K.G. and I.P. would like to thank the ICTP for hospitality during their stay where this work was started. The work of B.B. has been supported by the Slovenian Research Agency. The work of D.K.G. has been partially supported by the Department of Science and Technology, India under grant SR/S2/HEP-12/2006. The work of T.H. is supported by the U.S. Department of Energy under grant

No. DE-FG02-95ER40896. The work of G.-Y.H. is supported by the U.S. Department of Energy under grant No. DE-FG02-91ER40674 and by the U.C. Davis HEFTI program. The work of I.P. is supported by the Croatian Ministry of Science, Education and Sport under grant No. 023-0982887-3064. The work of G.S. is partially supported by the EU FP6 Marie Curie Research & Training Network ‘‘UniverseNet’’ (MRTN-CT-2006-035863).

APPENDIX A: HEAVY LEPTONS IN TYPE III SEESAW MODEL

1. The Lagrangian

We start with the Lagrangian of the SM leptons, i.e the three generations of left-handed doublet L_i and right-handed singlet e_i^c

$$L_i = \begin{pmatrix} \nu_i \\ e_i \end{pmatrix}, \quad e_i^c,$$

and an $SU(2)_L$ vector-like triplet T with zero hypercharge, plus a leptonic singlet S :

$$T^k = (T^1, T^2, T^3) \equiv \left(\frac{T^- + T^+}{\sqrt{2}}, \frac{T^- - T^+}{i\sqrt{2}}, T^0 \right), \quad S.$$

In the two-component notation, we write

$$\begin{aligned} \mathcal{L}_{kin} = & \bar{L}_j i \bar{\sigma}^\mu \left(\partial_\mu + ig' \frac{1}{2} B_\mu - ig \frac{\tau^a}{2} A_\mu^a \right) L_j + \bar{e}_j^c i \bar{\sigma}^\mu (\partial_\mu - ig' B_\mu) e_j^c \\ & + \bar{T}^k i \bar{\sigma}^\mu (\partial_\mu T^k - g \epsilon^{akj} A_\mu^a T^j) + \bar{S} i \bar{\sigma}^\mu \partial_\mu S. \end{aligned} \quad (\text{A1})$$

with $\bar{\sigma}^\mu = (1, \sigma^i)$, where σ^i are the Pauli matrices.

One can add to this Lagrangian Majorana mass terms for the triplet and singlet

$$\mathcal{L}_M = -\frac{M_T}{2} (2T^+ T^- + T^0 T^0) - \frac{M_S}{2} S S + h.c. \quad (\text{A2})$$

With properly defined T^k and S the masses M_T and M_S can be made real and positive.

The Yukawa terms are written as

$$\mathcal{L}_Y = -y_E^i H^\dagger e_i^c L_i + y_T^i H^T i \tau^2 \tau^a T^a L_i + y_S^i H^T i \tau^2 S L_i + h.c. \quad (\text{A3})$$

where y_E^i are the physical (real and diagonal) charged lepton Yukawas. After the spontaneous symmetry breaking of $SU(2)_L \times U(1)_Y$, working in the Unitary gauge,

$$H \rightarrow \begin{pmatrix} 0 \\ v + h/\sqrt{2} \end{pmatrix}, \quad (\text{A4})$$

with $v \approx 174$ GeV, we have the Yukawa terms (A3) written as

$$\mathcal{L}_Y \rightarrow - \left(v + \frac{h}{\sqrt{2}} \right) \left(y_E^i e_i^c e_i + y_T^i \left(\sqrt{2} T^+ e_i + T^0 \nu_i \right) + y_S^i S \nu_i \right) + h.c. \quad (\text{A5})$$

The electroweak gauge interactions of the fermions in (A1) are thus written as

$$\begin{aligned} \mathcal{L}_{gauge} = & e A_\mu \left(-\bar{e}_j \bar{\sigma}^\mu e_j + \bar{e}_j^c \bar{\sigma}^\mu e_j^c + \bar{T}^+ \bar{\sigma}^\mu T^+ - \bar{T}^- \bar{\sigma}^\mu T^- \right) \\ & + \frac{e Z_\mu}{2 s_w c_w} \left(\bar{\nu}_j \bar{\sigma}^\mu \nu_j + (2 s_w^2 - 1) \bar{e}_j \bar{\sigma}^\mu e_j - 2 s_w^2 \bar{e}_j^c \bar{\sigma}^\mu e_j^c \right. \\ & \quad \left. + 2 c_w^2 \bar{T}^+ \bar{\sigma}^\mu T^+ - 2 c_w^2 \bar{T}^- \bar{\sigma}^\mu T^- \right) \\ & + \frac{e}{s_w} W_\mu^+ \left(\frac{1}{\sqrt{2}} \bar{\nu}_j \bar{\sigma}^\mu e_j + \bar{T}^0 \bar{\sigma}^\mu T^- - \bar{T}^+ \bar{\sigma}^\mu T^0 \right) \\ & + \frac{e}{s_w} W_\mu^- \left(\frac{1}{\sqrt{2}} \bar{e}_j \bar{\sigma}^\mu \nu_j + \bar{T}^- \bar{\sigma}^\mu T^0 - \bar{T}^0 \bar{\sigma}^\mu T^+ \right), \end{aligned} \quad (\text{A6})$$

where

$$B_\mu = c_w A_\mu - s_w Z_\mu, \quad A_\mu^1 = \frac{W_\mu^- + W_\mu^+}{\sqrt{2}}, \quad (\text{A7})$$

$$A_\mu^3 = s_w A_\mu + c_w Z_\mu, \quad A_\mu^2 = \frac{W_\mu^- - W_\mu^+}{i\sqrt{2}}, \quad (\text{A8})$$

and $c_w \equiv \cos \theta_w$, $s_w \equiv \sin \theta_w$, $e = g s_w = g' c_w$.

2. Fermion mass eigenstates

The mass terms for the neutral fermions are

$$-\frac{1}{2} \begin{pmatrix} \nu_i & T^0 & S \end{pmatrix} \begin{pmatrix} 0 & v y_T^i & v y_S^i \\ v y_T^j & M_T & 0 \\ v y_S^j & 0 & M_S \end{pmatrix} \begin{pmatrix} \nu_j \\ T^0 \\ S \end{pmatrix} + h.c. \quad (\text{A9})$$

The symmetric complex 5×5 mass matrix can be diagonalized by a unitary transformation

$$\begin{pmatrix} \nu_j \\ T^0 \\ S \end{pmatrix} \rightarrow U_0 \begin{pmatrix} \nu_j \\ T^0 \\ S \end{pmatrix}. \quad (\text{A10})$$

In the leading order for $|v y_{T,S}^i| \ll M_{T,S}$, the unitary matrix is

$$U_0 \approx \begin{pmatrix} 1_{3 \times 3} & \epsilon_T^* & \epsilon_S^* \\ -\epsilon_T^T & 1 & 0 \\ -\epsilon_S^T & 0 & 1 \end{pmatrix}, \quad \epsilon_X^i = \frac{v y_X^i}{M_X}. \quad (\text{A11})$$

After this transformation the mass terms of the neutral fields become approximately

$$-\frac{1}{2}M_T T^0 T^0 - \frac{1}{2}M_S S S - \frac{1}{2}m_{ij}^\nu \nu_i \nu_j, \quad (\text{A12})$$

with

$$m_{ij}^\nu = -M_T \epsilon_T^i \epsilon_T^j - M_S \epsilon_S^i \epsilon_S^j. \quad (\text{A13})$$

The neutrino mass matrix gets diagonalized with the final transformation

$$\nu \rightarrow U_{PMNS} \nu. \quad (\text{A14})$$

The mass matrix for charged fermions is

$$-\begin{pmatrix} e_i^c & T^+ \end{pmatrix} \begin{pmatrix} m_E^i \delta_{ij} & 0 \\ \nu y_T^j & M_T \end{pmatrix} \begin{pmatrix} e_j \\ T^- \end{pmatrix} + h.c. \quad , \quad m_E^i \equiv \nu y_E^i. \quad (\text{A15})$$

This 4×4 complex mass matrix can be diagonalized by two unitary matrices:

$$\begin{pmatrix} e_j \\ T^- \end{pmatrix} \rightarrow U_- \begin{pmatrix} e_j \\ T^- \end{pmatrix}, \quad \begin{pmatrix} e_j^c \\ T^+ \end{pmatrix} \rightarrow U_+ \begin{pmatrix} e_j^c \\ T^+ \end{pmatrix}. \quad (\text{A16})$$

In the same approximation as before and for $|m_E^i| \ll M_T$

$$U_- \approx \begin{pmatrix} 1_{3 \times 3} & \sqrt{2} \epsilon_T^* \\ -\sqrt{2} \epsilon_T^T & 1 \end{pmatrix}, \quad U_+ \approx 1. \quad (\text{A17})$$

3. Interaction in the mass eigenbasis

We will eventually be interested in the decay rates of the triplets into a light lepton and a gauge boson. These go through one power of the small Dirac Yukawa couplings y_T^i . It is thus sufficient at leading order to make the following substitutions in (A6), coming from (A10)–(A11)

$$\nu_j \rightarrow \nu_j + \epsilon_T^{j*} T^0 + \epsilon_S^{j*} S, \quad T^0 \rightarrow T^0 - \epsilon_T^k \nu_k, \quad S \rightarrow S - \epsilon_S^k \nu_k, \quad (\text{A18})$$

and (A16)–(A17)

$$e_j \rightarrow e_j + \sqrt{2} \epsilon_T^{j*} T^-, \quad T^- \rightarrow T^- - \sqrt{2} \epsilon_T^k e_k. \quad (\text{A19})$$

All the fields on the right-hand sides except the light neutrinos are the mass eigenstates, i.e. the asymptotic states in scattering and decays. Neutrinos in final states will be always summed over all three generations, so their true basis is irrelevant. Equation (A6) gets some new terms, that come from mixings:

$$\begin{aligned} \delta\mathcal{L}_{gauge} = & \frac{eZ_\mu}{2s_w c_w} \left(\epsilon_T^j \overline{T^0} \bar{\sigma}^\mu \nu_j + \sqrt{2} \epsilon_T^j \overline{T^-} \bar{\sigma}^\mu e_j + \epsilon_S^j \overline{S} \bar{\sigma}^\mu \nu_j \right) \\ & + \frac{e}{s_w} W_\mu^+ \left(\epsilon_T^j \overline{T^+} \bar{\sigma}^\mu \nu_j - \frac{1}{\sqrt{2}} \epsilon_T^j \overline{T^0} \bar{\sigma}^\mu e_j + \frac{1}{\sqrt{2}} \epsilon_S^j \overline{S} \bar{\sigma}^\mu e_j \right) + h.c. \end{aligned} \quad (\text{A20})$$

4. Interaction in the four component notation

For some convenience, we rewrite the Lagrangian in four-component notation, in which the Dirac fields are

$$e_j = \begin{pmatrix} e_j \\ \bar{e}_{c_j} \end{pmatrix}, \quad T^- = \begin{pmatrix} T^- \\ \overline{T^+} \end{pmatrix}, \quad (\text{A21})$$

and the Majorana fields are

$$\nu_j = \begin{pmatrix} \nu_j \\ \bar{\nu}_j \end{pmatrix}, \quad T^0 = \begin{pmatrix} T^0 \\ \overline{T^0} \end{pmatrix}. \quad (\text{A22})$$

Keeping in mind our convention [48] (see also [49])

$$\gamma^\mu = \begin{pmatrix} 0 & \sigma^\mu \\ \bar{\sigma}^\mu & 0 \end{pmatrix}, \quad \gamma^5 = \begin{pmatrix} 1 & 0 \\ 0 & -1 \end{pmatrix}, \quad \sigma^\mu = (1, -\sigma^i), \quad (\text{A23})$$

and using the relation

$$\bar{\psi} \bar{\sigma}^\mu \chi = -\chi \sigma^\mu \bar{\psi} \quad (\text{A24})$$

with ψ and χ two-component spinors, the quadratic terms are rewritten in the four-component notation as

$$\mathcal{L}_{kin} = \bar{e}_j i \gamma^\mu \partial_\mu e_j + \overline{T^-} (i \gamma^\mu \partial_\mu - M_T) T^- + \frac{1}{2} \bar{\nu}_j i \gamma^\mu \partial_\mu \nu_j + \frac{1}{2} \overline{T^0} (i \gamma^\mu \partial_\mu - M_T) T^0, \quad (\text{A25})$$

where we assume that all SM light charged leptons and neutrinos are massless. Before mixing the gauge interactions (A6) become

$$\begin{aligned} \mathcal{L}_{gauge} = & -e A_\mu (\bar{e}_j \gamma^\mu e_j + \overline{T^-} \gamma^\mu T^-) \\ & + \frac{e}{2s_w c_w} Z_\mu (\bar{\nu}_j \gamma^\mu P_+ \nu_j + (2s_w^2 - 1) \bar{e}_j \gamma^\mu P_+ e_j + 2s_w^2 \bar{e}_j \gamma^\mu P_- e_j - 2c_w^2 \overline{T^-} \gamma^\mu T^-) \\ & + \frac{e}{s_w} W_\mu^+ \left(\frac{1}{\sqrt{2}} \bar{\nu}_j \gamma^\mu P_+ e_j + \overline{T^0} \gamma^\mu T^- \right) + \frac{e}{s_w} W_\mu^- \left(\frac{1}{\sqrt{2}} \bar{e}_j \gamma^\mu P_+ \nu_j + \overline{T^-} \gamma^\mu T^0 \right), \end{aligned} \quad (\text{A26})$$

	v_C	a_C	v_E	a_E	v_N	a_N
triplet	$\sqrt{2}$	0	$-2 \cos^2 \theta_W$	0	0	0
vector-like doublet	1	0	$-1 + 2 \sin^2 \theta_W$	0	1	0
sequential doublet	1/2	1/2	$-1/2 + 2 \sin^2 \theta_W$	-1/2	1/2	1/2

TABLE IV: Electroweak couplings of the extra leptons.

with the projection operators defined as $P_{\pm} = (1 \pm \gamma^5)/2$ for the left-handed (+) and right-handed (-) chiralities.

The extra terms (A20) are put in the form

$$\begin{aligned} \delta \mathcal{L}_{gauge} = & \frac{e}{2s_w c_w} Z_{\mu} \left(\epsilon_T^j \bar{T}^0 \gamma^{\mu} P_+ \nu_j + \sqrt{2} \epsilon_T^j \bar{T}^- \gamma^{\mu} P_+ e_j + \epsilon_S^j \bar{S} \gamma^{\mu} P_+ \nu_j \right) \\ & + \frac{e}{s_w} W_{\mu}^+ \left(-\epsilon_T^j \bar{\nu}_j \gamma^{\mu} P_- T^- - \frac{1}{\sqrt{2}} \epsilon_T^j \bar{T}^0 \gamma^{\mu} P_+ e_j + \frac{1}{\sqrt{2}} \epsilon_S^j \bar{S} \gamma^{\mu} P_+ e \right) + h.c. \end{aligned} \quad (\text{A27})$$

One can transform to the four component notation also the Yukawa interactions (A5). The pieces new with respect to the SM are

$$\delta \mathcal{L}_Y = -\frac{h}{\sqrt{2}} \left(\sqrt{2} y_T^j \bar{T}^- P_+ e_j + y_T^j \bar{\nu}_j P_+ T^0 + y_S^j \bar{\nu}_j P_+ S \right) + h.c. \quad (\text{A28})$$

5. Comparison of heavy leptons gauge couplings

In this appendix, we list the heavy lepton couplings to the SM gauge bosons. We denote a generic charged lepton by E (with charge -1), and a neutral lepton by N . We first neglect the small mixings with the SM leptons and write the gauge couplings in a form

$$\begin{aligned} \mathcal{L} = & \frac{g}{\sqrt{2}} W^{+\mu} \bar{N} \gamma_{\mu} (v_C + a_C \gamma_5) E + h.c. \\ & + \frac{g}{2 \cos \theta_W} Z^{\mu} (\bar{E} \gamma_{\mu} (v_E + a_E \gamma_5) E + \bar{N} \gamma_{\mu} (v_N + a_N \gamma_5) N) \end{aligned} \quad (\text{A29})$$

The vector and axial couplings are summarized in Table. IV.

For off-diagonal couplings between a heavy lepton and a SM lepton, simply include a mixing such as ϵ_T^i .

APPENDIX B: PRODUCTION CROSS SECTIONS AND DECAY RATES

1. Production cross sections

$$\underline{f\bar{f} \rightarrow E^+E^-}$$

The Drell-Yan mechanism $f\bar{f} \rightarrow E^+E^-$, with E^\pm is a heavy lepton, proceed through photon and Z boson s -channel exchange. The corresponding differential cross section is found to be:

$$\frac{d\sigma}{d\Omega} = \frac{\beta}{64\pi^2 s} \frac{1}{4} \frac{1}{N_c} (|M_\gamma|^2 + |M_Z|^2 + 2\Re(M_\gamma^* M_Z)) \quad (\text{B1})$$

with

$$\begin{aligned} |M_\gamma|^2 &= 4Q_f^2 Q_E^2 e^4 [(1 + \cos^2 \theta) + (1 - \cos^2 \theta)\gamma^{-2}] \\ |M_Z|^2 &= \frac{g^4}{4 \cos^4 \theta_W} \frac{s^2}{(s - m_Z^2)^2} [8a_f v_f a_E v_E \beta \cos \theta \\ &\quad + (a_f^2 + v_f^2)\{(a_E^2 \beta^2 + v_E^2)(1 + \cos^2 \theta) + v_E^2(1 - \cos^2 \theta)\gamma^{-2}\}] \end{aligned} \quad (\text{B2})$$

$$\Re(M_\gamma^* M_Z) = Q_f Q_E \frac{e^2 g^2}{\cos^2 \theta_W} \frac{s}{s - m_Z^2} [2a_f a_E \beta \cos \theta + v_f v_E \{(1 + \cos^2 \theta) + (1 - \cos^2 \theta)\gamma^{-2}\}]$$

where N_c is a color factor and is 1 (3) for f is a lepton (quark). θ is the scattering angle of E^+ with respect to the f beam direction, $\beta = \sqrt{1 - 4M_E^2/s}$ is the speed of the outgoing particle in the CM frame, with $\gamma^{-2} = 4M_E^2/s$. The coupling of the heavy lepton to Z boson are listed in Table IV while the SM coupling of Z to initial states fermions are given by:

$$\begin{aligned} v_e &= -1/2 - 2Q_e \sin^2 \theta_W, \quad v_d = -1/2 - 2Q_d \sin^2 \theta_W, \quad v_u = 1/2 - 2Q_u \sin^2 \theta_W \\ a_e &= -1/2, \quad a_d = -1/2, \quad a_u = 1/2 \end{aligned}$$

with $Q_e = -1$, $Q_d = -1/3$ and $Q_u = 2/3$

$$\underline{f\bar{f}' \rightarrow W^* \rightarrow E^+N^0}$$

The production mechanism $f\bar{f}' \rightarrow E^+N$, with E^\pm is a heavy charged lepton and N a neutral one, proceed through W^\pm boson s -channel exchange. The differential cross section is:

$$\begin{aligned} \frac{d\sigma}{d\Omega} &= \frac{\beta}{64\pi^2 s} \frac{1}{4} \frac{1}{N_c} g^4 \frac{s^2}{(s - m_W^2)^2} [8v_f^2 v_C a_C \beta \cos \theta \\ &\quad + 2v_f^2 \{(a_C^2 \beta^2 + v_C^2)(1 + \cos^2 \theta) + v_C^2(1 - \cos^2 \theta)(1 - \beta^2)\}] \end{aligned} \quad (\text{B3})$$

with $v_f = a_f = 1/2$, V_C and a_C are given in Table IV.

$$\underline{f\bar{f}' \rightarrow W^* \rightarrow N^0 l_j^\pm}$$

The production mechanism $f'\bar{f} \rightarrow N^0 l_j^\pm$, with N^0 is a heavy neutral lepton proceed through W^\pm boson s -channel exchange. The differential cross section is:

$$\frac{d\sigma}{d\Omega} = \frac{\beta}{64\pi^2 s} \frac{1}{4} \frac{1}{N_c} g^4 \frac{s^2}{(s - m_W^2)^2} [8a_f a_C v_f v_C \cos\theta + \beta(v_f^2 + a_f^2)(2 + \cos^2\theta - \beta^2)(a_C^2 + v_C^2)] \quad (\text{B4})$$

with $v_f = a_f = 1/2$, $V_C = a_C = 1/2\epsilon_T^j$, and θ is the scattering angle of N^0 with respect to the f beam direction.

$$\underline{f\bar{f} \rightarrow Z^* \rightarrow E^\mp l_j^\pm}$$

The production mechanism $f\bar{f} \rightarrow E^\mp l_j^\pm$, with E^\pm is a heavy charged lepton proceed through Z boson s -channel exchange. The differential cross section is the same as Eq. (B4) with the following replacements: $g \rightarrow g/(\sqrt{2}\cos\theta_W)$, $m_W \rightarrow m_Z$, $M_N \rightarrow M_E$, $v_f \rightarrow v_{u,d}$, $a_f \rightarrow a_{u,d}$ and $a_C = v_C = 1/\sqrt{2}\epsilon_T^j$

2. Decay widths for $T \rightarrow W, Z, h +$ light lepton

If kinematically accessible, the predominant decay modes of the triplet leptons will be to the gauge bosons (or a Higgs boson) plus a SM light lepton, whose coupling strength is

dictated by the neutral Dirac Yukawa couplings. Those decay widths are listed below [22]:

$$\sum_k \Gamma(T^- \rightarrow W^- \nu_k) = \frac{M_T}{16\pi} \left(\sum_k |y_T^k|^2 \right) \left(1 - \frac{m_W^2}{M_T^2} \right)^2 \left(1 + 2 \frac{m_W^2}{M_T^2} \right), \quad (\text{B5})$$

$$\Gamma(T^- \rightarrow Z e_k^-) = \frac{M_T}{32\pi} |y_T^k|^2 \left(1 - \frac{m_Z^2}{M_T^2} \right)^2 \left(1 + 2 \frac{m_Z^2}{M_T^2} \right), \quad (\text{B6})$$

$$\Gamma(T^- \rightarrow h e_k^-) = \frac{M_T}{32\pi} |y_T^k|^2 \left(1 - \frac{m_h^2}{M_T^2} \right)^2, \quad (\text{B7})$$

$$\begin{aligned} \Gamma(T^0 \rightarrow W^+ e_k^-) &= \Gamma(T^0 \rightarrow W^- e_k^+) = \\ &= \frac{M_T}{32\pi} |y_T^k|^2 \left(1 - \frac{m_W^2}{M_T^2} \right)^2 \left(1 + 2 \frac{m_W^2}{M_T^2} \right), \end{aligned} \quad (\text{B8})$$

$$\sum_k \Gamma(T^0 \rightarrow Z \nu_k) = \frac{M_T}{32\pi} \left(\sum_k |y_T^k|^2 \right) \left(1 - \frac{m_Z^2}{M_T^2} \right)^2 \left(1 + 2 \frac{m_Z^2}{M_T^2} \right), \quad (\text{B9})$$

$$\sum_k \Gamma(T^0 \rightarrow h \nu_k) = \frac{M_T}{32\pi} \left(\sum_k |y_T^k|^2 \right) \left(1 - \frac{m_h^2}{M_T^2} \right)^2, \quad (\text{B10})$$

where we averaged over initial polarizations and summed over final ones.

-
- [1] S. Weinberg, Phys. Rev. Lett. **43** (1979) 1566.
- [2] E. Ma, Phys. Rev. Lett. **81** (1998) 1171 [arXiv:hep-ph/9805219].
- [3] P. Minkowski, Phys. Lett. B **67** (1977) 421; T. Yanagida, proceedings of the *Workshop on Unified Theories and Baryon Number in the Universe*, Tsukuba, 1979, eds. A. Sawada, A. Sugamoto; S. Glashow, in *Cargese 1979, Proceedings, Quarks and Leptons* (1979); M. Gell-Mann, P. Ramond, R. Slansky, proceedings of the *Supergravity Stony Brook Workshop*, New York, 1979, eds. P. Van Nieuwenhuizen, D. Freeman; R. Mohapatra, G. Senjanović, Phys. Rev. Lett. **44** (1980) 912.
- [4] M. Magg and C. Wetterich, Phys. Lett. B **94** (1980) 61;
- [5] G. Lazarides, Q. Shafi and C. Wetterich, Nucl. Phys. B **181** (1981) 287;
- [6] R. N. Mohapatra and G. Senjanović, Phys. Rev. D **23** (1981) 165.
- [7] R. Foot, H. Lew, X. G. He and G. C. Joshi, Z. Phys. C **44** (1989) 441.
- [8] J. C. Pati and A. Salam, Phys. Rev. D **10**, 275 (1974) [Erratum-ibid. D **11**, 703 (1975)].
- [9] R. N. Mohapatra and J. C. Pati, Phys. Rev. D **11**, 566 (1975).
- [10] G. Senjanović and R. N. Mohapatra, Phys. Rev. D **12**, 1502 (1975).

- [11] G. Senjanović, Nucl. Phys. B **153**, 334 (1979).
- [12] B. Bajc and G. Senjanović, JHEP **0708** (2007) 014 [arXiv:hep-ph/0612029].
- [13] W. Y. Keung and G. Senjanović, Phys. Rev. Lett. **50**, 1427 (1983).
- [14] E. Ma and D. P. Roy, Nucl. Phys. B **644** (2002) 290 [arXiv:hep-ph/0206150].
- [15] R. Franceschini, T. Hambye and A. Strumia, Phys. Rev. D **78** (2008) 033002 [arXiv:0805.1613 [hep-ph]].
- [16] F. del Aguila and J. A. Aguilar-Saavedra, arXiv:0808.2468 [hep-ph].
- [17] F. del Aguila and J. A. Aguilar-Saavedra, arXiv:0809.2096 [hep-ph].
- [18] H. Georgi and S. L. Glashow, Phys. Rev. Lett. **32** (1974) 438.
- [19] P. J. Fox *et al.*, arXiv:hep-th/0503249.
- [20] I. Doršner and P. Fileviez Perez, Nucl. Phys. B **723** (2005) 53 [arXiv:hep-ph/0504276].
- [21] I. Doršner, P. Fileviez Perez and R. Gonzalez Felipe, Nucl. Phys. B **747** (2006) 312 [arXiv:hep-ph/0512068].
- [22] B. Bajc, M. Nemevšek and G. Senjanović, Phys. Rev. D **76**, 055011 (2007) [arXiv:hep-ph/0703080].
- [23] P. Q. Hung, Phys. Lett. B **649** (2007) 275 [arXiv:hep-ph/0612004].
- [24] S. B. Gudnason, T. A. Ryttov and F. Sannino, Phys. Rev. D **76** (2007) 015005 [arXiv:hep-ph/0612230].
- [25] E. Ma, Phys. Lett. B **625** (2005) 76 [arXiv:hep-ph/0508030].
- [26] T. Schwetz, AIP Conf. Proc. **981**, 8 (2008) [arXiv:0710.5027 [hep-ph]].
- [27] J. A. Casas and A. Ibarra, Nucl. Phys. B **618** (2001) 171 [arXiv:hep-ph/0103065].
- [28] A. Ibarra and G. G. Ross, Phys. Lett. B **591**, 285 (2004) [arXiv:hep-ph/0312138].
- [29] W. L. Guo, Z. Z. Xing and S. Zhou, Int. J. Mod. Phys. E **16** (2007) 1 [arXiv:hep-ph/0612033].
- [30] A. Abada, C. Biggio, F. Bonnet, M. B. Gavela and T. Hambye, Phys. Rev. D **78** (2008) 033007 [arXiv:0803.0481 [hep-ph]].
- [31] X. G. He and S. Oh, arXiv:0902.4082 [hep-ph].
- [32] A. Arhrib, R. Benbrik and C. H. Chen, arXiv:0903.1553 [hep-ph].
- [33] J. Kamenik and M. Nemevšek, to appear.
- [34] C. Amsler *et al.* [Particle Data Group], Phys. Lett. B **667** (2008) 1.
- [35] M. Ibe, T. Moroi and T. T. Yanagida, Phys. Lett. B **644** (2007) 355 [arXiv:hep-ph/0610277].
- [36] A. Strumia and F. Vissani, arXiv:hep-ph/0606054.

- [37] CTEQ Collaboration, J. Pumplin, D. R. Stump, J. Huston, H. L. Lai, P. M. Nadolsky and W. K. Tung, JHEP **0207**, 012 (2002) [arXiv:hep-ph/0201195].
- [38] T. Han and B. Zhang, Phys. Rev. Lett. **97** (2006) 171804 [arXiv:hep-ph/0604064]; A. Atre, T. Han, S. Pascoli and B. Zhang, arXiv:0901.3589 [hep-ph].
- [39] F. del Aguila, J. A. Aguilar-Saavedra and R. Pittau, JHEP **0710** (2007) 047 [arXiv:hep-ph/0703261].
- [40] K. Cheung and C. W. Chiang, Phys. Rev. D **71** (2005) 095003 [arXiv:hep-ph/0501265].
- [41] V. M. Abazov *et al.* [D0 Collaboration], Phys. Rev. Lett. **99** (2007) 191802 [arXiv:hep-ex/0702005].
- [42] P. Fileviez Perez, T. Han, G. Y. Huang, T. Li and K. Wang, Phys. Rev. D **78** (2008) 015018 [arXiv:0805.3536 [hep-ph]].
- [43] D. E. Acosta *et al.* [CDF Collaboration], Phys. Rev. D **71**, 052003 (2005) [arXiv:hep-ex/0410041]; V. M. Abazov *et al.* [D0 Collaboration], Nucl. Instrum. Meth. A **565**, 463 (2006) [arXiv:physics/0507191].
- [44] G. L. Bayatian *et al.* [CMS Collaboration], J. Phys. G **34**, 995 (2007); G. Aad *et al.* [ATLAS Collaboration], arXiv:0901.0512.
- [45] J. Alwall, P. Demin, S. de Visscher, R. Frederix, M. Herquet, F. Maltoni, T. Plehn, D.L. Rainwater and T. Stelzer, JHEP **0709** (2007) 028 [arXiv:0706.2334 [hep-ph]].
- [46] G. D. Kribs, T. Plehn, M. Spannowsky and T. M. P. Tait, Phys. Rev. D **76** (2007) 075016 [arXiv:0706.3718 [hep-ph]]; W. S. Hou, arXiv:0803.1234 [hep-ph].
- [47] G. Weiglein *et al.* [LHC/LC Study Group], Phys. Rept. **426** (2006) 47 [arXiv:hep-ph/0410364].
- [48] J. P. Derendinger, “Lecture Notes On Globally Supersymmetric Theories In Four-Dimensions And Two-Dimensions,” in Proceedings of the Hellenic School of Particle Physics, Corfu, Greece, September 1989, edited by G. Zoupanos and N. Tracas; also available at http://www.unine.ch/phys/hepth/Derend/SUSY_nd.pdf.
- [49] H. K. Dreiner, H. E. Haber and S. P. Martin, arXiv:0812.1594 [hep-ph].